

# piRNAs regulate a Hedgehog germline-to-soma pro-aging signal

Received: 26 August 2021

Accepted: 3 November 2022

Published online: 9 January 2023

 Check for updatesCheng Shi<sup>1,2</sup>✉ & Coleen T. Murphy<sup>1</sup>✉

The reproductive system regulates somatic aging through competing anti- and pro-aging signals. Germline removal extends somatic lifespan through conserved pathways including insulin and mammalian target-of-rapamycin signaling, while germline hyperactivity shortens lifespan through unknown mechanisms. Here we show that mating-induced germline hyperactivity downregulates piRNAs, in turn desilencing their targets, including the Hedgehog-like ligand-encoding genes *wrt-1* and *wrt-10*, ultimately causing somatic collapse and death. Germline-produced Hedgehog signals require PTR-6 and PTR-16 receptors for mating-induced shrinking and death. Our results reveal an unconventional role of the piRNA pathway in transcriptional regulation of Hedgehog signaling and a new role of Hedgehog signaling in the regulation of longevity and somatic maintenance: Hedgehog signaling is controlled by the tunable piRNA pathway to encode the previously unknown germline-to-soma pro-aging signal. Mating-induced piRNA downregulation in the germline and subsequent Hedgehog signaling to the soma enable the animal to tune somatic resource allocation to germline needs, optimizing reproductive timing and survival.

Longevity is plastic and is influenced by external factors, for example, diet, and internal factors such as reproductive demands. Communication between the germline and soma allows a coordinated response to physiological and environmental challenges. Animals couple nutrient availability to reproduction<sup>1</sup>, a typical example of soma-to-germline communication, through conserved signaling pathways, including the insulin, AMP-activated protein kinase (AMPK), and mammalian target-of-rapamycin (mTOR) pathways<sup>2–6</sup>. Conversely, the status of worm, fly, mouse, and human germlines influence their somatic tissues: germline removal and ovary transplantation extend lifespan<sup>7–11</sup>, while germline hyperactivity decreases lifespan and leads to dramatic changes in somatic physiology in animals across great evolutionary distances<sup>12–14</sup>. While these studies in animals ranging from invertebrates to humans support the existence of a pro-aging signal from the germlines, the nature and identity of that signal remains elusive.

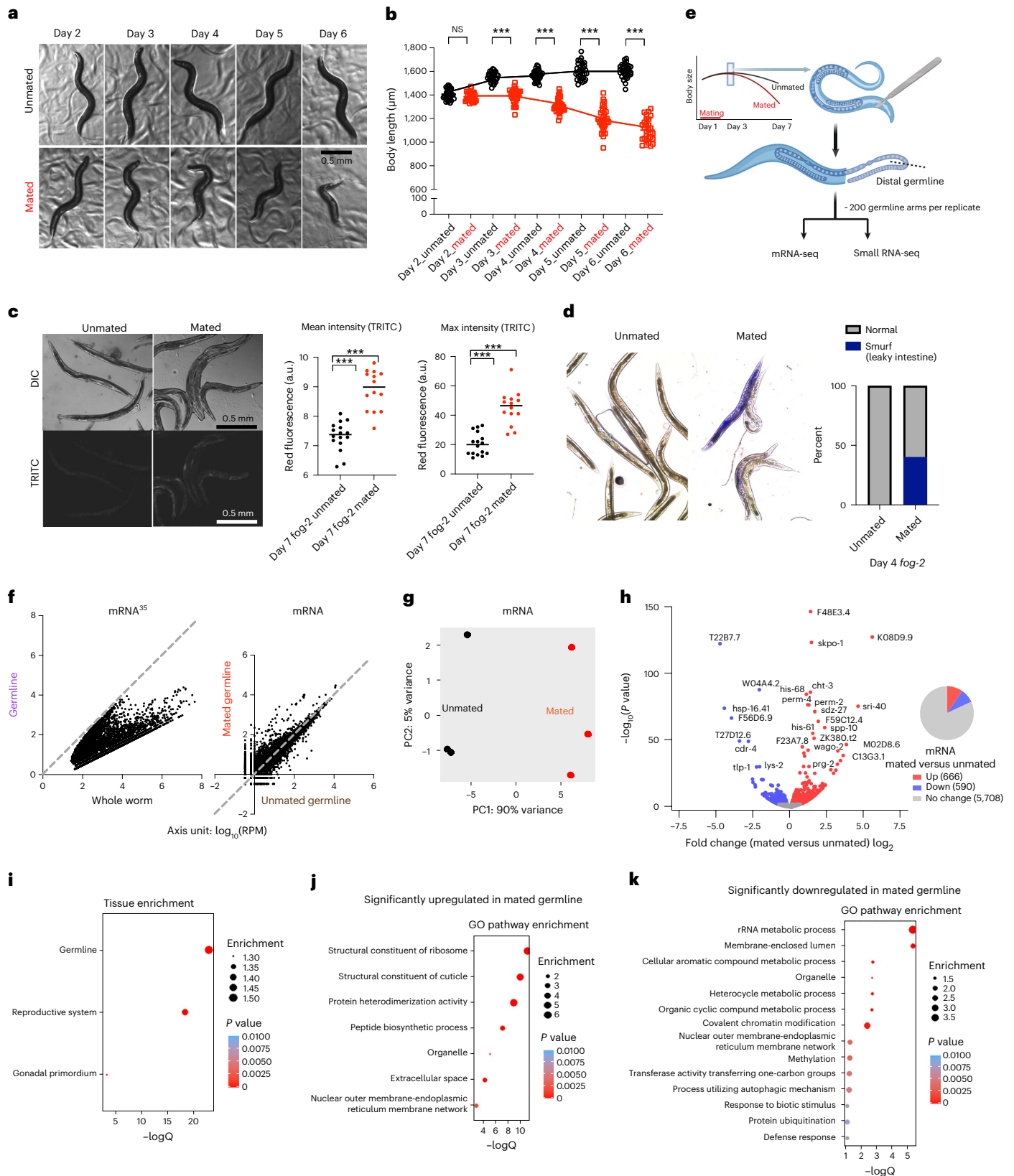
Removal of the germline extends lifespan, increases fat accumulation, and enhances resistance to various stresses<sup>7,10,15–18</sup>. However, concomitant removal of the somatic gonad eliminates lifespan extension and other somatic benefits, suggesting the existence of two opposing

signals: a germline pro-aging signal and a somatic gonad prolongevity signal<sup>7,19</sup>. The somatic gonad prolongevity signal pathway has been characterized using germlineless worms<sup>20–28</sup>. Dafachronic acids, insulin, mTOR, and steroid signaling are required in the soma for germline loss-mediated lifespan regulation, suggesting that they mediate the somatic gonad prolongevity effect<sup>11,19–21,24,29,30</sup>. By contrast, the identity of the initial pro-aging signal originating from the germline remains elusive. Identifying this pro-aging signal is critical for understanding how animals tune their aging rates in response to germline activity and reproductive needs.

While most studies of the influence of germline on lifespan have compared germlineless animals with intact, unmated animals<sup>7,19</sup>, less is known about the role of the hyperactive germline. Mating accelerates germline proliferation and ultimately leads to somatic collapse, shrinking and early death<sup>12,13</sup>, suggesting that the germline pro-aging signal is substantially amplified by mating. Therefore, mated worms are an ideal system in which to identify the mysterious germline pro-aging signal.

We set out to identify the underlying mechanism of hyperactive germline-induced shrinking and early death. Our transcriptional

<sup>1</sup>Department of Molecular Biology and Lewis-Sigler Institute for Integrative Genomics, Princeton University, Princeton, NJ, USA. <sup>2</sup>Present address: Department of Biological Sciences, University of New Orleans, New Orleans, LA, USA. ✉e-mail: [cshi@uno.edu](mailto:cshi@uno.edu); [ctmurphy@princeton.edu](mailto:ctmurphy@princeton.edu)



analyses of isolated germlines revealed that a specific subset of piRNAs is downregulated in response to mating, de-repressing Hedgehog-related genes. Hedgehog signaling communicates the status of the germline to somatic cells, resulting in mating-induced shrinking and early death. Thus, somatic responses to germline hyperactivity are tuned by piRNA regulation of an important developmental signaling pathway.

## Results

### Mating induces transcriptional changes in the germline

Mating causes shrinking and decreased lifespan<sup>12</sup>. Day 1 adult self-spermless hermaphrodites (*fog-2*) mated for 24 h with Day 1 adult males live 40% shorter than their unmated counterparts, and shrink by up to 30%<sup>12</sup> (Fig. 1a,b and Extended Data Fig. 1a,b). (*fog-2*) hermaphrodites, the

**Fig. 1 | Mating induces shrinking and significant transcriptional changes in the germline.** **a**, Representative images of the unmated and mated hermaphrodites from Day 2–6 of adulthood. Mating occurs on Day 1 for 24 h. **b**, Length of unmated and mated *fog-2* hermaphrodites. Day 2 unmated,  $1,407 \pm 45 \mu\text{m}$  ( $n = 30$ ); Day 2 mated,  $1,386 \pm 39 \mu\text{m}$  ( $n = 30$ );  $P = 0.0642$ . Day 3 unmated,  $1,552 \pm 41 \mu\text{m}$  ( $n = 30$ ); Day 3 mated,  $1,392 \pm 59 \mu\text{m}$  ( $n = 30$ );  $P < 0.0001$ . Day 4 unmated,  $1,568 \pm 44 \mu\text{m}$  ( $n = 30$ ); Day 4 mated,  $1,309 \pm 59 \mu\text{m}$  ( $n = 30$ );  $P < 0.0001$ . Day 5 unmated,  $1,604 \pm 69 \mu\text{m}$  ( $n = 30$ ); Day 5 mated,  $1,194 \pm 100 \mu\text{m}$  ( $n = 30$ );  $P < 0.0001$ . Day 6 unmated,  $1,603 \pm 59 \mu\text{m}$  ( $n = 30$ ); Day 6 mated,  $1,102 \pm 95 \mu\text{m}$  ( $n = 29$ );  $P < 0.0001$ ;  $***P < 0.0001$ , NS, no statistical difference. Body size data are presented as mean body length  $\pm$  s.d. for all body size measurements in this study;  $n$ , number of biologically independent animals for all body size measurements. Two-tailed  $t$ -test was used for all body size measurement comparisons in this study. **c**, Autofluorescence (red) is significantly increased by mating. Left, representative images of Day 7 mated and unmated *fog-2* hermaphrodites; right, quantification of mean and maximum red autofluorescence (via tetramethylrhodamine isothiocyanate (TRITC) filterset). Unmated mean,  $7.3 \pm 0.5$  ( $n = 16$ ); mated mean,  $8.9 \pm 0.7$  ( $n = 14$ ) arbitrary units (a.u.);  $P < 0.0001$ . Unmated max,  $20.4 \pm 7.6$  ( $n = 16$ ); mated max,  $45.1 \pm 11.5$  ( $n = 14$ ) a.u.;  $P < 0.0001$ . Red autofluorescence data are presented as mean/maximum values  $\pm$  s.d.;  $n$  represents the number of biologically independent animals. Two-tailed  $t$ -test was used to determine the statistical significance.  $***P < 0.0001$ . DIC, differential interference contrast. **d**, Mating induces breakdown of intestinal

barrier function. Left, representative images of Day 4 mated and unmated *fog-2* hermaphrodites after soaking in blue dye overnight; right, quantification of intestinal leakage in the population of mated and unmated worms. **e**, Experimental design of germline isolation from mated and unmated *fog-2* hermaphrodites. **f**, Left, over 8,000 mRNAs express at a lower level in the distal germline compared with whole animals (regraphed using published data<sup>35</sup>). Right, expression levels in mated and unmated germlines (mRNA-seq data from this study) for the same set of mRNAs as on the left. Axis unit,  $\log_{10}$ (RPM). **g**, PCA of normalized read counts from the mRNA transcriptomes of the isolated germlines. **h**, Volcano plot of mRNA-seq transcriptome data displaying the pattern of gene expression values for mated versus unmated germlines. Significantly differentially-expressed genes (adjusted  $P$  value ( $P_{\text{adj}}$ )  $\leq 0.05$ ) are highlighted in red (upregulation) and blue (downregulation), whereas genes with no significant expression changes are in gray. The pie chart (right) summarizes the number of significantly differentially-expressed genes in the mated germline compared with the unmated germline.  $P$  values are calculated in DESeq2 using the Wald test. Full list of genes for **h** is available as Source Data. **i**, Tissue enrichment analysis of significantly differentially-expressed genes in the mated germline (<https://wormbase.org/tools/enrichment/tea/tea.cgi>). **j, k**, GO enrichment analysis of significantly up- (**j**) and down- (**k**) regulated genes in the mated germline (<https://wormbase.org/tools/enrichment/tea/tea.cgi>).  $P$  values in **i–k** were calculated by a hypergeometric function after FDR correction using a Benjamini–Hochberg algorithm as previously described<sup>86</sup>.

control genotype, are self-spermless; successful mating can be determined quickly by the presence of fertilized eggs inside the worm.) In addition to shrinking, mated animals also display an acceleration in age-related autofluorescence<sup>31</sup> and intestinal barrier dysfunction (Fig. 1c,d); this phenomenon is specific to mating, as developmentally small *sma-9* mutants do not exhibit these defects (Extended Data Fig. 1c–e) and still shrink upon mating (Extended Data Fig. 1f)<sup>12</sup>. The longevity decrease after mating is mediated by multiple factors, including seminal fluid transfer, male sperm-induced germline hyperactivity, and male pheromone toxicity<sup>12,13,32–34</sup>. While seminal fluid-mediated death involves insulin-like peptides and the insulin/FOXO signaling pathway, the germline-specific pro-aging signal that induces shrinking is unknown<sup>12</sup>.

To identify the germline pro-aging signal that induces postmating physiological changes and early death, we dissected distal germlines from mated and unmated hermaphrodites, and performed mRNA sequencing (mRNA-seq) and small RNA sequencing (RNA-seq) (Fig. 1e). Hermaphrodites were mated with young males from Day 1 of adulthood for 2 days before germline dissection. Because mating causes a significant reduction of the mitotic distal germline region (about 30% decrease in size and 40% decrease in nuclei number<sup>12</sup>), we used an equal amount of RNA, rather than an equal number of worms or germline, from each germline sample to make our sequencing libraries, and sequencing reads were normalized in our analysis. In unmated

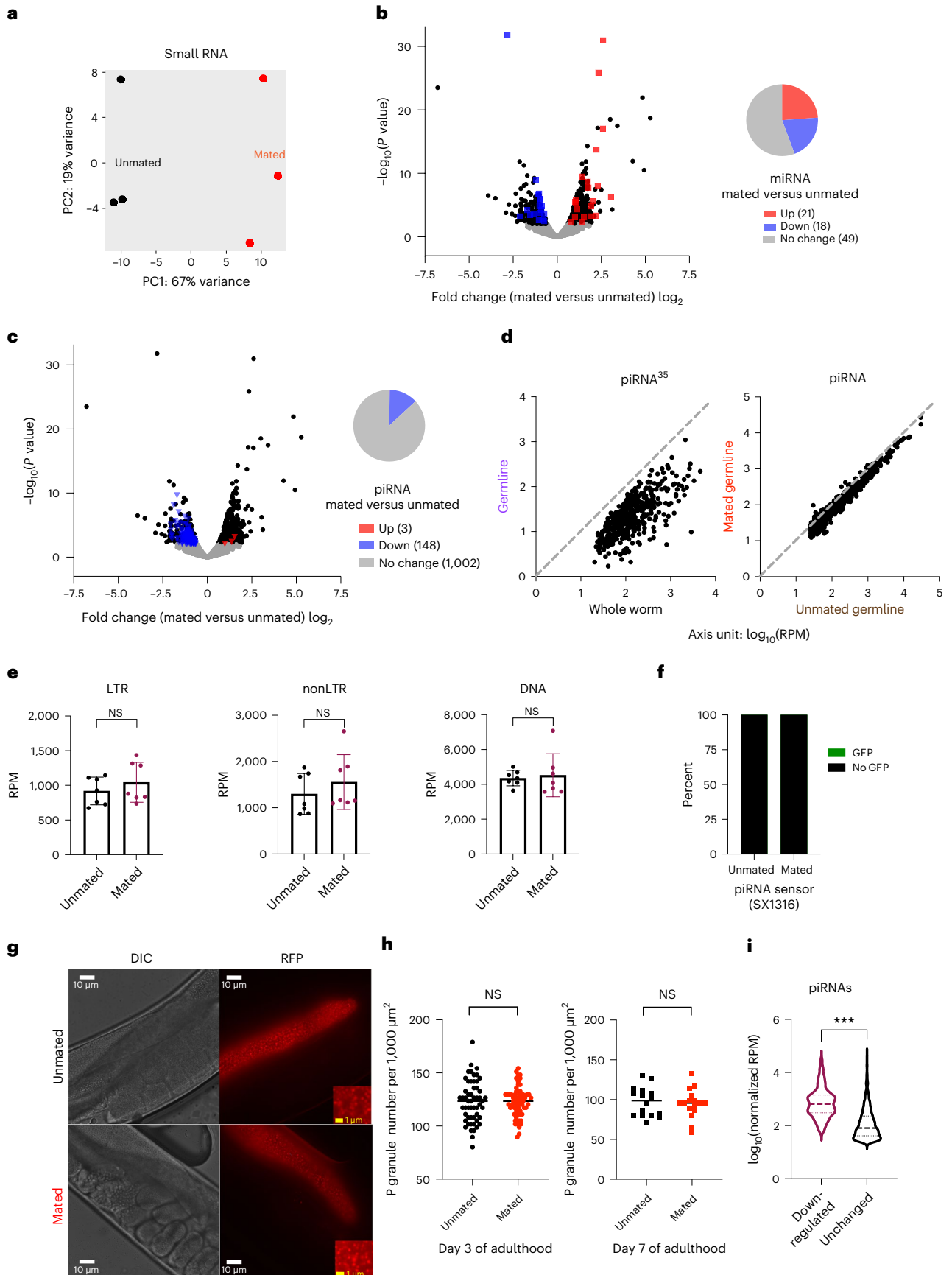
hermaphrodites, over 8,000 mRNAs were previously reported to have reduced expression in the distal germline compared with whole animals<sup>35</sup> (Fig. 1f, left). These distal germline-depleted genes in unmated worms were not enriched in the mated germline (Fig. 1f, right). Therefore, the significantly differentially-expressed genes we identified here are induced specifically by mating rather than by reduction in size of the mated germline.

A total of 666 genes were significantly differentially upregulated and 590 were downregulated in mated germlines compared with unmated germlines (Fig. 1g,h and Source Data). These genes were enriched in germline, reproductive system and gonadal primordium function, confirming successful dissection of the germline with minimum contamination by other tissues (Fig. 1i). Upregulated mated germline genes were enriched for ribosome, cuticle, protein heterodimerization and peptide biosynthesis (Fig. 1j), which are essential for rapid germ cell proliferation and cellularization. One of the most upregulated genes, *sri-40* (Fig. 1h), was also significantly induced in whole body after mating with males and, when reduced, extends lifespan with and without males, suggesting its involvement in general protection of mating-induced death<sup>34</sup>. Genes downregulated in the mated germline include metabolic processes (rRNA, cellular aromatic compound and heterocycle metabolic process) (Fig. 1k), indicating a shift of metabolic activities in the mated germline.

**Fig. 2 | Mating downregulates a small and specific set of piRNAs without a general disruption of the piRNA pathway.**

**a**, PCA of normalized read counts from the small RNA transcriptomes of the isolated germlines. **b, c**, Volcano plots of small RNA-seq transcriptome data of mated versus unmated germlines. Black dots, significantly differentially-expressed small RNAs (full list is available as Source Data); gray dots, small RNAs with no significant expression changes after mating. Significantly differentially-expressed miRNAs (**b**) or piRNAs (**c**) ( $P_{\text{adj}} \leq 0.05$ ) are highlighted in red (upregulation) and blue (downregulation). The pie chart (right) summarizes the number of significantly differentially-expressed and unchanged miRNAs (**b**) or piRNAs (**c**) in the mated germline compared with the unmated germline. **d**, Left, over 1,000 piRNAs express at a lower level in the distal germline compared with whole animals (regraphed using published data<sup>35</sup>). Right, expression levels in mated and unmated germlines (small RNA-seq data from this study) for the same set of piRNAs as on the left. Axis unit,  $\log_{10}$ (RPM). **e**, Mating does not change levels of main types of TE (Source Data). Seven biological replicates in total. LTR (left) unmated,  $919 \pm 200$  RPM; mated,  $1,044 \pm 289$  RPM;  $P = 0.3624$ ; nonLTR (middle) unmated,  $1,299 \pm 444$  RPM;

mated,  $1,556 \pm 593$  RPM;  $P = 0.3761$ ; DNA (right) unmated,  $4,360 \pm 445$  RPM; mated,  $4,527 \pm 1,240$  RPM;  $P = 0.7432$ . Expression levels are presented as mean values  $\pm$  s.d. Two-tailed  $t$ -test was used to determine statistical significance. NS, no statistical difference. **f**, The general piRNA sensor (SX1316) remains silenced in mated worms; 25 worms were checked for each condition. **g, h**, Mating does not affect the morphology or density of P granules. **g**, Representative images of mated and unmated Day 3 Y968 worms (P granules labeled by PGL-1::RFP). Mating started on Day 1 for 2 days. **h**, Quantification of P granule density (blindly scored) of Day 3 (left) and Day 7 (right) worms: Day 3 unmated,  $123 \pm 20$  per  $1,000 \mu\text{m}^2$  ( $n = 55$ ); mated,  $123 \pm 14$  per  $1,000 \mu\text{m}^2$  ( $n = 63$ );  $P = 0.9363$ . Day 7 unmated,  $97 \pm 18$  per  $1,000 \mu\text{m}^2$  ( $n = 16$ ); mated,  $95 \pm 18$  per  $1,000 \mu\text{m}^2$  ( $n = 16$ );  $P = 0.7217$ . Data are presented as mean values  $\pm$  s.d.;  $n$ , number of biologically independent germlines. Two-tailed unpaired  $t$ -test was used to determine statistical significance. **i**, Mating-induced downregulated piRNAs are expressed at a significantly higher level in the unmated germline compared with the other over 1,000 unchanged piRNAs.  $***P < 0.0001$ ; two-tailed unpaired  $t$ -test was used to determine statistical significance.



### piRNAs are downregulated in the mated germline

Several species of small RNAs are expressed primarily in the germline and regulate germline function. For example, microRNAs are critical in lifespan regulation after germline removal<sup>27,36</sup>. Endogenous siRNAs are required for maintenance of proteostasis and lifespan extension in germlineless worms<sup>37</sup>, and play critical roles in shaping the germline transcriptome<sup>35</sup>. PIWI-associated RNAs (piRNAs) are expressed predominantly in the germline and are required to maintain germline integrity and fertility<sup>38</sup>. Differential expression analysis of small RNAs from dissected mated and unmated germlines revealed 440 significantly upregulated and 296 downregulated small RNAs in the mated germline (Fig. 2a and Source Data). Whereas miRNAs showed equal distribution in up- and downregulation (Fig. 2b), a small set of piRNAs were almost exclusively (98%) downregulated in the mated germline (148 downregulated versus 3 upregulated; Fig. 2c), indicating that mating triggers a unique response in germline piRNA abundance. While many species of small RNAs, including over 1,500 piRNAs, are depleted in the distal germline compared with the whole worm in unmated hermaphrodites<sup>35</sup> (Fig. 2d, left), we do not see a general bias in piRNA expression; that is, these piRNAs were not enriched in the mated germline (Fig. 2d, right), suggesting that mating-induced downregulation of specific piRNAs is not due simply to the reduction of the mitotic germline region caused by mating.

The best-characterized function of piRNAs is the silencing of transposable elements (TE) to preserve genome integrity<sup>39,40</sup>. We observed that the main classes of TE were expressed at similar levels in unmated and mated germlines (Fig. 2e and Source Data), suggesting that piRNA changes are unlikely to be regulating TE in this context. In addition, mated and unmated worms showed no difference in activity of a general piRNA sensor, that is, desilenced if the piRNA pathway is completely nonfunctional<sup>41,42</sup> (Fig. 2f). P granules are essential for piRNA-mediated gene silencing<sup>43</sup>; however, neither P granule density nor morphology was changed immediately after mating (Day 3) or when shrinking is obvious (Day 7) (Fig. 2g,h), suggesting that general piRNA function in P granules is not affected by mating. Moreover, although we detected more than 1,000 piRNAs in our dissected germlines that were unchanged upon mating (Fig. 2c), these specific 148 mating-induced downregulated piRNAs were expressed at a significantly higher levels in the unmated germline compared with the other over 1,000 unchanged

piRNAs (Fig. 2i). Together, our data suggest that mating leads to the downregulation of a small and specific set of piRNAs without a general disruption of the piRNA pathway.

### Mating-induced changes require the germline piRNA pathway

To further test which types of small RNA are required for germline-specific mating-induced response, we measured body size changes after mating for different types of small RNA pathway mutants, as shrinking serves as a phenotypic readout for the germline-emanating pro-aging signal<sup>12</sup>. We mated mutant hermaphrodites with young males for 2 days starting on Day 1 of adulthood and measured their body size on Day 6/7 of adulthood (Extended Data Fig. 2a). DCR-1 is required for both miRNA and siRNA processing<sup>44–46</sup>. Like wildtype animals, after mating, *dcr-1* hermaphrodites still shrank (Fig. 3a and Extended Data Fig. 2a), suggesting that Dicer function is unnecessary for the germline-to-soma shrinking signal. ALG-3 and ALG-4 are Argonaute proteins that bind and stabilize 26G siRNAs in the germline and mediate their effector functions<sup>47,48</sup>; *alg-3;alg-4* double mutants still shrank after mating (Fig. 3a). Likewise, mutants of the dsRNA transporter SID-1 were also susceptible to mating-induced shrinking (Fig. 3a), suggesting that mating-induced shrinking does not rely on functional endogenous small RNA pathways.

Next, we tested mutants for factors in the piRNA pathway, including piRNA transcription (*prde-1* (ref. 49)), maturation (*prg-1* (refs. 50–52)), secondary amplification (*ekl-1*, *drh-3* (refs. 41, 53)), and nuclear silencing (*hpl-2* (ref. 54)), as well as MAGO12, which has loss-of-function mutations in multiple Argonaute protein-encoding genes<sup>53</sup>. Unlike the mutants involved in siRNA processing (Fig. 3a), none of these piRNA pathway mutants shrank after mating (Fig. 3b–d and Extended Data Fig. 2a), indicating that the piRNA pathway is required for mating-induced shrinking in the hermaphrodites. Moreover, one genomic copy of the secondary amplification genes *ekl-1* and *drh-3* restored the susceptibility of worms to mating-induced shrinking (indicated by '+/–'; Fig. 3c). Together, our data suggest that piRNA pathway function is critical for the signal that conveys the mated state of the germline to the soma.

piRNAs scan most of the transcriptome while located in P granules (*Caenorhabditis elegans* germ granules)<sup>43,55,56</sup>, and disruption of P granules compromises piRNA-mediated silencing<sup>43</sup>. P granule distribution and assembly/disassembly dynamics depend on maternal-effect germline (MEG) proteins<sup>57</sup>. We found that *meg* double mutants in

### Fig. 3 | Mating-induced shrinking and transcriptional changes require the functional piRNA pathway in the germline. a–f, Body size measurements of mated and unmated hermaphrodites related to different small RNA pathways. a, Mutants that are defective in miRNA or siRNA pathways still shrink after mating. N2 unmated, 1,334 ± 81 μm (n = 30); N2 mated, 1,088 ± 122 μm (n = 31); \*\*\*P < 0.001. *dcr-1(mg375)* unmated, 1,347 ± 84 μm (n = 30); mated, 1,088 ± 122 μm (n = 30); \*\*\*P < 0.001. *sid-1(qt9)* unmated, 1,102 ± 78 μm (n = 20); mated, 898 ± 101 μm (n = 21); \*\*\*P < 0.001. *fog-2(q71)* unmated, 1,436 ± 54 μm (n = 30); mated, 1,099 ± 128 μm (n = 22); \*\*\*P < 0.001. *alg-4(ok1041); alg-3(tm1155)* unmated, 1,364 ± 78 μm (n = 25); mated, 1,060 ± 136 μm (n = 25); \*\*\*P < 0.001. b–f, Mutants in which multiple steps of the piRNA pathway are affected are resistant to mating-induced shrinking. b, piRNA pathway mutants do not shrink after mating. *fog-2(q71)* unmated, 1,546 ± 55 μm (n = 30); mated, 1,065 ± 127 μm (n = 30); \*\*\*P < 0.001. *prg-1(n4357)* unmated, 1,368 ± 100 μm (n = 30); mated, 1,369 ± 114 μm (n = 30); P = 0.9603. *prde-1(mj207)* unmated, 1,385 ± 106 μm (n = 30); mated, 1,376 ± 120 μm (n = 31); P = 0.7581. c, *ekl-1* and *drh-3* mutant alleles are maintained by chromosome balancers. Postmating body size of siblings with homozygous mutant alleles (–/–, no balancer) and heterozygous mutant allele (+/–, with the balancer) was measured in the same experiment. *ekl-1(ok1197)[+/-]* unmated, 1,306 ± 105 μm (n = 25); mated, 1,039 ± 140 μm (n = 20); \*\*\*P < 0.001. *ekl-1(ok1197)[-/-]* unmated, 1,464 ± 87 μm (n = 16); mated, 1,460 ± 111 μm (n = 16); P = 0.9063. *drh-3(tm1217)[+/-]* unmated, 1,247 ± 117 μm (n = 21); mated, 951 ± 58 μm (n = 16); \*\*\*P < 0.001. *drh-3(tm1217)[-/-]* unmated, 1,294 ± 104 μm (n = 16); mated, 1,321 ± 58 μm (n = 5); P = 0.5863. d, *fog-2(q71)* unmated, 1,422 ± 69 μm (n = 30); mated, 1,122 ± 125 μm (n = 30); \*\*\*P < 0.001. *hpl-2(ok916)* unmated, 1,215 ± 130 μm (n = 30); mated, 1,212 ± 164 μm (n = 30); P = 0.9286.

MAGO12 unmated, 1,365 ± 65 μm (n = 30); mated, 1,361 ± 100 μm (n = 30); P = 0.8577. e, *fog-2(q71)* unmated, 1,349 ± 73 μm (n = 25); mated, 1,151 ± 89 μm (n = 25); \*\*\*P < 0.001. *meg-3(tm4259) meg-4(ax2026)* unmated, 1,312 ± 71 μm (n = 25); mated, 1,289 ± 161 μm (n = 25); P = 0.5179. *meg-1(vr10) meg-3(tm4259)* unmated, 1,298 ± 89 μm (n = 25); mated, 1,311 ± 104 μm (n = 25); P = 0.6330. f, N2 unmated, 1,191 ± 40 μm (n = 25); mated, 1,078 ± 69 μm (n = 25); \*\*\*P < 0.001. *Cer1(-)* (RNAi for three generations) unmated, 1,170 ± 46 μm (n = 25); mated, 1,081 ± 59 μm (n = 25); \*\*\*P < 0.001. TEI, transgenerational epigenetic inheritance. g, Mating induces shrinking in hermaphrodites with germline-specific rescue of the piRNA pathway. *fog-2(q71)* unmated, 1,462 ± 68 μm (n = 25); mated, 1,189 ± 131 μm (n = 25); \*\*\*P < 0.001. *prg-1(n4357)* unmated, 1,322 ± 96 μm (n = 20); mated, 1,363 ± 101 μm (n = 25); P = 0.1803. Germline-specific *prg-1* rescue (CQ655) unmated, 1,431 ± 74 μm (n = 25); mated, 1,212 ± 152 μm (n = 25); \*\*\*P < 0.001. h, Summary of the genetic requirement for mating-induced shrinking. i, PCA of normalized read counts from the mRNA transcriptomes of the isolated germlines. Black, *fog-2* unmated; red, *fog-2* mated; gray, *prde-1* unmated; pink, *prde-1* mated. Full list of mating-induced significantly differentially-expressed genes in *prde-1* germline is available as Source Data. j, Quantification of maximum value of *Pdaf-9::daf-9::gfp* expression in the spermatheca in wildtype (left) and *prde-1* (right) background. All measurements were normalized to the DAF-9 expression in the XXX cells in the head, which is not affected by mating. Unmated control, 44.1 ± 17.0 a.u. (n = 11); mated control, 25.7 ± 11.7 a.u. (n = 13); P = 0.0049; unmated *prde-1*, 34.4 ± 7.4 a.u. (n = 13); mated *prde-1*, 31.7 ± 4.2 a.u. (n = 14); P = 0.2676. Data are presented as maximum values ± s.d.; n, number of biologically independent animals. Two-tailed t-test was used to determine statistical significance. \*\*P < 0.01.

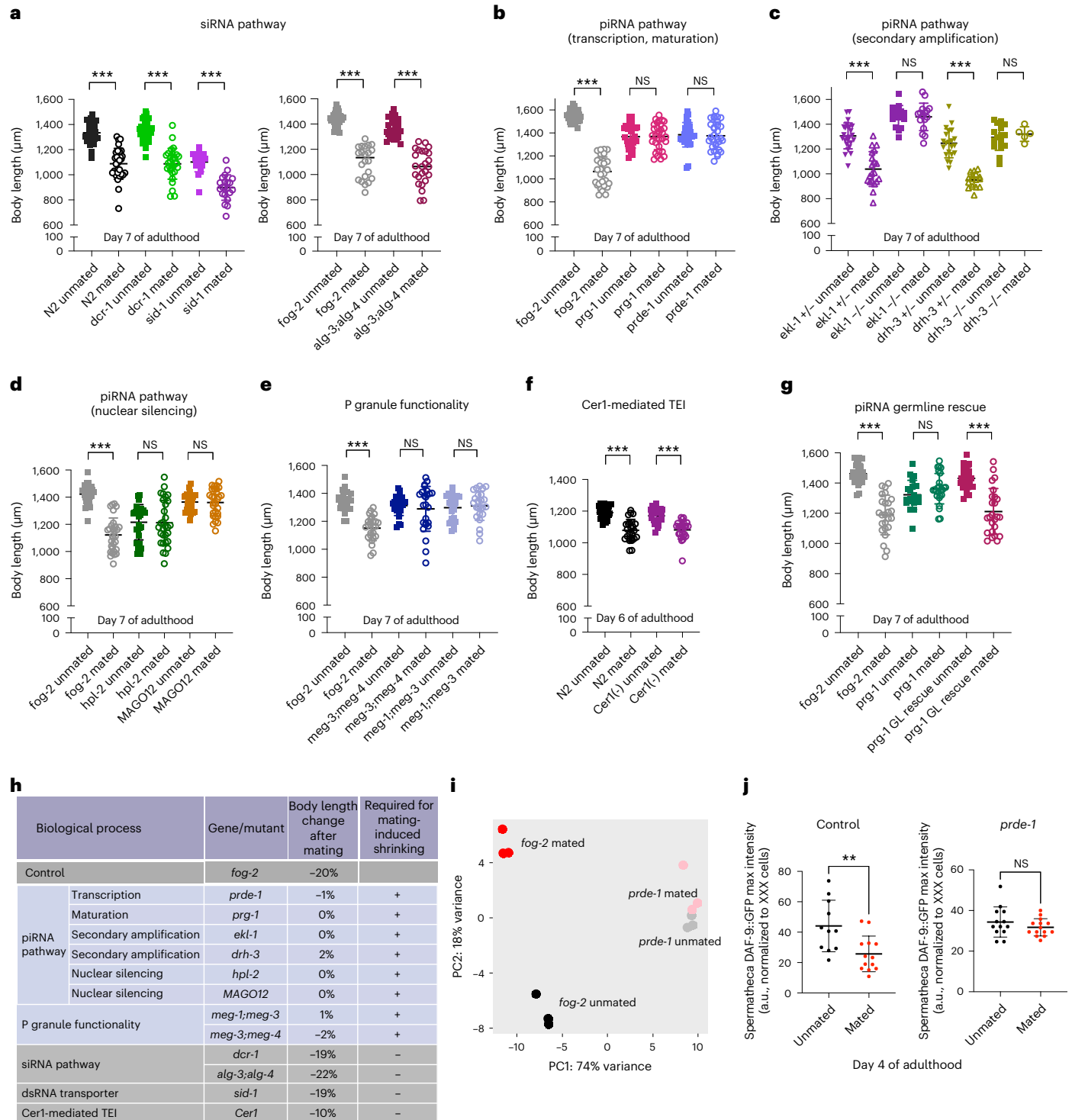
which P granule functionality is severely impaired<sup>57</sup> were also resistant to mating-induced shrinking (Fig. 3e), demonstrating again that the germline-mediated postmating shrinking requires a functional piRNA pathway and P granules.

We recently found that the *Cer1* retrotransposon is required for communication between the germline and neurons in the transgenerational inheritance of pathogen avoidance, which also requires the germline and piRNAs<sup>58</sup>. However, worms lacking *Cer1* retrotransposon-encoded capsids still shrank after mating (Fig. 3f), suggesting that *Cer1* is not involved in mating-induced shrinking.

Although piRNAs are expressed predominantly in the germline, the piRNA pathway also functions in somatic tissue<sup>59</sup>. To determine

whether the piRNA pathway is required in the germline to mediate mating-induced shrinking, we tested a germline-specific *prg-1* rescue strain; mating induced shrinking in these animals (Fig. 3g), confirming that piRNA function in the germline is sufficient to mediate postmating shrinking (Fig. 3h).

Next, we wondered whether the piRNA pathway is required for the dramatic mRNA transcriptional changes in mated germlines. To address this question, we isolated mated and unmated distal germlines from *prde-1* mutants, which are defective in piRNA biosynthesis<sup>49</sup>, and performed mRNA-seq. Principal component analysis (PCA) revealed that the lack of a functional piRNA pathway in *prde-1* worms eliminated most germline transcriptional differences induced by mating



(Source Data, Fig. 3i and Extended Data Fig. 2b,c). *Prde-1* mutation eliminated the upregulation of genes in mated germlines (Extended Data Fig. 2b), indicating that the mating-induced transcriptional changes in the germline are also dependent on a functional piRNA pathway.

We previously found that *daf-9* and *daf-12* are required for mating-induced shrinking and that DAF-9::GFP is reduced after mating in spermatheca<sup>12</sup>. However, in the *prde-1* background, we did not observe mating-induced reduction of DAF-9::GFP signal, suggesting that *prde-1* and piRNA regulation lie upstream of the spermatheca and *daf-9* regulation (Fig. 3j).

### Hedgehog signaling may be the mysterious pro-aging signal

Both postmating shrinking and transcriptional changes require piRNA pathway function, implying that the germline pro-aging signal must be related to piRNAs. Since the pro-aging signal is amplified in mated germlines, but specific piRNAs are downregulated, piRNAs themselves are unlikely to be the direct signal. Nor did we observe expression differences in TE between unmated and mated germlines (Fig. 2e), suggesting that piRNA regulation of TE is unlikely to be the signal. Therefore, we hypothesized that the mating-induced pro-aging process may be regulated through another main role of piRNAs, endogenous gene silencing<sup>60</sup>. Mating-induced downregulation of piRNAs may release the silencing effect on specific piRNA targets, upregulating the expression of these genes, making piRNAs' targeted genes more likely candidates for the germline pro-aging signal.

Reasoning that the pro-aging signal should be amplified after mating, we started with the list of 666 genes that are significantly

upregulated in the mated germlines we identified in our mRNA-seq analysis (Fig. 4a). Since the pro-aging signal originates from the germline, it must be germline-specific; we subtracted those genes that are also upregulated in mated *glp-1* germlineless worms<sup>34</sup> from the original list, reducing the number of candidates to 418 (Source Data, Fig. 4a and Extended Data Fig. 2d). Next, we reasoned that the amplified germline signal should be robust enough to be identified in the transcriptome of whole worms with an intact germline, since the germline accounts for a significant proportion of the whole worm biomass. We compared these 418 genes with our previous *fog-2* mated versus unmated whole-worm expression data<sup>61</sup> and found that the two datasets share 117 genes (Supplementary Data 1). Furthermore, since piRNAs are required for mating-induced transcriptional changes and shrinking, the germline signal should also be dependent on piRNAs. Therefore, we compared the remaining 117 genes with potential predicted targets (using the default 'relaxed' piRNA targeting setting from piRTarBase<sup>62</sup>) of 148 significantly downregulated piRNAs identified in the mated germline (Supplementary Data 2); 34 of 117 genes were targets predicted to be regulated by the 148 piRNAs that were downregulated in mated germline (Supplementary Data 3). Finally, to relay the signal from the germline to the rest of the body, the gene product is likely to be secreted. We applied two prediction algorithms (Euk-mPloc 2.0 (ref. 63) and SignalP<sup>64</sup>) to the 34 genes and found that 13 are predicted to encode secreted proteins. We then ranked the final 13 genes according to their expression fold change in the germline and in the whole worm, and their consistency in expression patterns across the samples (Fig. 4b and Supplementary Data 3).

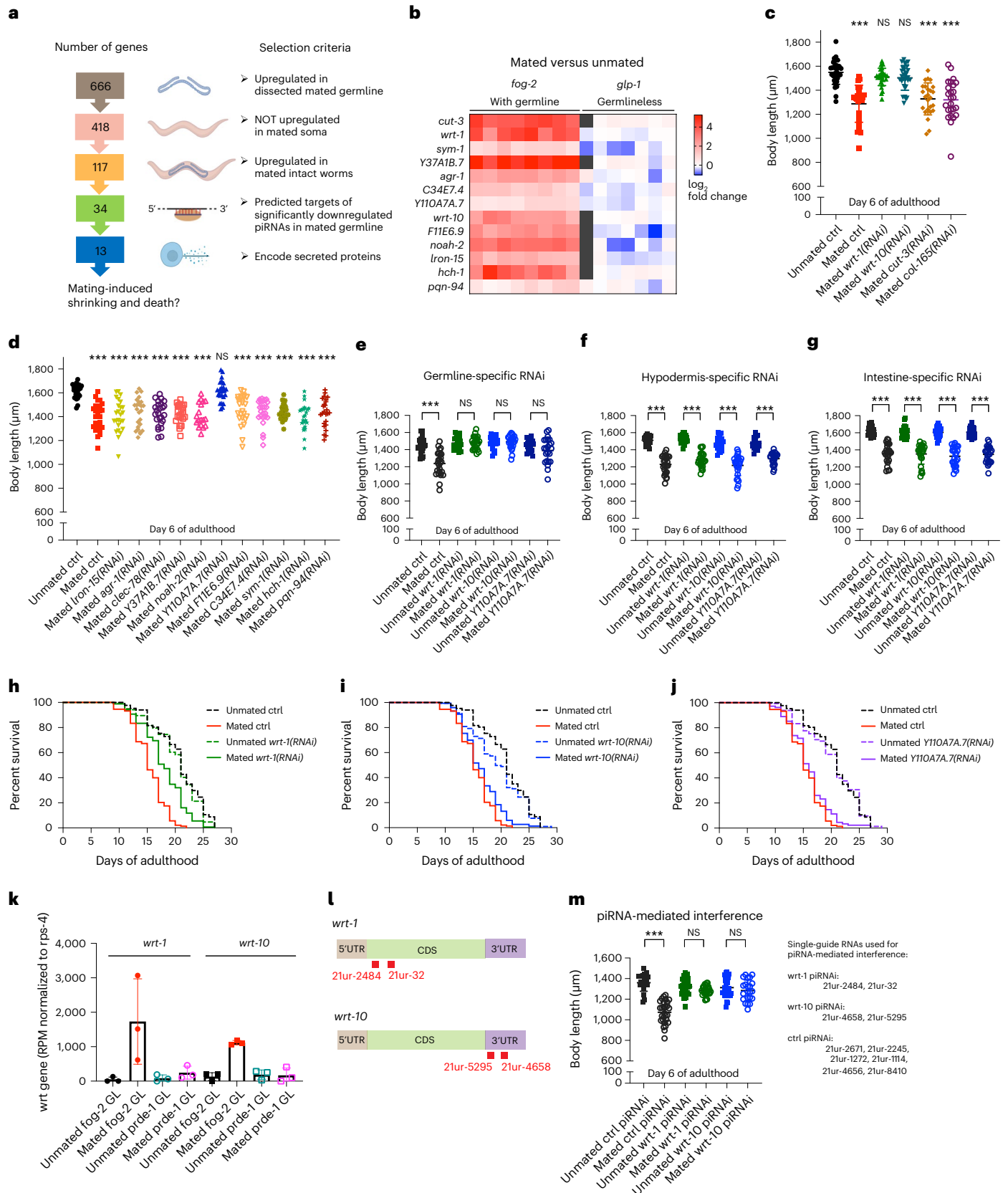
### Fig. 4 Secreted Hedgehog-like ligands in the germline are required for mating-induced shrinking and early death.

**a**, Scheme describing the strategy and criteria to narrow the list of genes (Source Data) that might encode the germline pro-aging signal. **b**, Heatmap of the final 13 germline pro-aging signal candidates. Their mating-induced upregulation is completely lost in mated germlineless worms. The data are displayed as  $\log_2(\text{fold change})$  of expression level in mated versus unmated whole worms. Left, *fog-2* worms with functional germlines; right, *glp-1* germlineless worms. **c,d**, Body size measurements of mated worms with RNAi treatment of individual candidate genes. **c**, *fog-2(q71)* unmated (control (ctrl) RNAi),  $1,549 \pm 99 \mu\text{m}$  ( $n = 30$ ); mated (control RNAi),  $1,288 \pm 155 \mu\text{m}$  ( $n = 25$ ); \*\*\* $P < 0.001$ ; mated *wrt-1(RNAi)*,  $1,511 \pm 72 \mu\text{m}$  ( $n = 27$ );  $P = 0.1070$ ; mated *wrt-10(RNAi)*,  $1,503 \pm 103 \mu\text{m}$  ( $n = 28$ );  $P = 0.0917$ ; mated *cut-3(RNAi)*,  $1,329 \pm 133 \mu\text{m}$  ( $n = 25$ ); \*\*\* $P < 0.001$ ; mated *col-165(RNAi)*,  $1,321 \pm 165 \mu\text{m}$  ( $n = 25$ ); \*\*\* $P < 0.001$ . **d**, *fog-2(q71)* unmated (control RNAi),  $1,615 \pm 58 \mu\text{m}$  ( $n = 25$ ); mated (control RNAi),  $1,404 \pm 116 \mu\text{m}$  ( $n = 25$ ); \*\*\* $P < 0.001$ ; mated *iron-15(RNAi)*,  $1,405 \pm 133 \mu\text{m}$  ( $n = 25$ ); \*\*\* $P < 0.001$ ; mated *agr-1(RNAi)*,  $1,433 \pm 124 \mu\text{m}$  ( $n = 25$ ); \*\*\* $P < 0.001$ ; mated *clec-78(RNAi)*,  $1,425 \pm 101 \mu\text{m}$  ( $n = 25$ ); \*\*\* $P < 0.001$ ; mated *Y37A1B.7(RNAi)*,  $1,421 \pm 78 \mu\text{m}$  ( $n = 25$ ); \*\*\* $P < 0.001$ ; mated *noah-2(RNAi)*,  $1,414 \pm 100 \mu\text{m}$  ( $n = 25$ ); \*\*\* $P < 0.001$ ; mated *Y110A7A.7(RNAi)*,  $1,615 \pm 85 \mu\text{m}$  ( $n = 25$ );  $P = 0.9780$ ; mated *F11E6.9(RNAi)*,  $1,461 \pm 124 \mu\text{m}$  ( $n = 25$ ); \*\*\* $P < 0.001$ ; mated *C34E7.4(RNAi)*,  $1,441 \pm 106 \mu\text{m}$  ( $n = 25$ ); \*\*\* $P < 0.001$ ; mated *sym-1(RNAi)*,  $1,441 \pm 66 \mu\text{m}$  ( $n = 25$ ); \*\*\* $P < 0.001$ ; mated *hch-1(RNAi)*,  $1,401 \pm 109 \mu\text{m}$  ( $n = 25$ ); \*\*\* $P < 0.001$ ; mated *pqn-94(RNAi)*,  $1,433 \pm 118 \mu\text{m}$  ( $n = 25$ ); \*\*\* $P < 0.001$ . **e-g**, Germline-specific knockdown (e) but not hypodermis-specific (f) or intestine-specific (g) knockdown of *wrt-1*, *wrt-10* and *Y110A7A.7* protects the mated hermaphrodites from shrinking. **e**, Germline-specific RNAi strain (DCL569) unmated (control RNAi),  $1,449 \pm 89 \mu\text{m}$  ( $n = 25$ ); mated (control RNAi),  $1,239 \pm 141 \mu\text{m}$  ( $n = 25$ ); \*\*\* $P < 0.001$ ; unmated *wrt-1(RNAi)*,  $1,477 \pm 71 \mu\text{m}$  ( $n = 25$ ); mated *wrt-1(RNAi)*,  $1,479 \pm 74 \mu\text{m}$  ( $n = 25$ );  $P = 0.9211$ ; unmated *wrt-10(RNAi)*,  $1,485 \pm 76 \mu\text{m}$  ( $n = 25$ ); mated *wrt-10(RNAi)*,  $1,491 \pm 77 \mu\text{m}$  ( $n = 25$ );  $P = 0.7701$ ; unmated *Y110A7A.7(RNAi)*,  $1,441 \pm 66 \mu\text{m}$  ( $n = 20$ ); mated *Y110A7A.7(RNAi)*,  $1,391 \pm 147 \mu\text{m}$  ( $n = 23$ );  $P = 0.1698$ . **f**, Hypodermis-specific RNAi strain (CQ479) unmated (control RNAi),  $1,511 \pm 51 \mu\text{m}$  ( $n = 22$ ); mated (control RNAi),  $1,230 \pm 105 \mu\text{m}$  ( $n = 26$ ); \*\*\* $P < 0.001$ ; unmated *wrt-1(RNAi)*,  $1,528 \pm 49 \mu\text{m}$  ( $n = 25$ ); mated *wrt-1(RNAi)*,  $1,282 \pm 83 \mu\text{m}$  ( $n = 25$ ); \*\*\* $P < 0.001$ ; unmated *wrt-10(RNAi)*,  $1,477 \pm 75 \mu\text{m}$  ( $n = 21$ ); mated *wrt-10(RNAi)*,  $1,218 \pm 120 \mu\text{m}$  ( $n = 26$ ); \*\*\* $P < 0.001$ ; unmated *Y110A7A.7(RNAi)*,  $1,474 \pm 67 \mu\text{m}$  ( $n = 17$ ); mated *Y110A7A.7(RNAi)*,  $1,297 \pm 67 \mu\text{m}$  ( $n = 24$ ); \*\*\* $P < 0.001$ . **g**, Intestine-specific RNAi strain (IG1839) unmated (control RNAi),  $1,627 \pm 53 \mu\text{m}$  ( $n = 25$ ); mated (control RNAi),  $1,357 \pm 111 \mu\text{m}$  ( $n = 25$ ); \*\*\* $P < 0.001$ ; unmated *wrt-1(RNAi)*,  $1,603 \pm 67 \mu\text{m}$

( $n = 25$ ); mated *wrt-1(RNAi)*,  $1,352 \pm 118 \mu\text{m}$  ( $n = 25$ ); \*\*\* $P < 0.001$ ; unmated *wrt-10(RNAi)*,  $1,605 \pm 58 \mu\text{m}$  ( $n = 25$ ); mated *wrt-10(RNAi)*,  $1,326 \pm 110 \mu\text{m}$  ( $n = 25$ ); \*\*\* $P < 0.001$ ; unmated *Y110A7A.7(RNAi)*,  $1,607 \pm 52 \mu\text{m}$  ( $n = 25$ ); mated *Y110A7A.7(RNAi)*,  $1,348 \pm 96 \mu\text{m}$  ( $n = 25$ ); \*\*\* $P < 0.001$ . **h-j**, RNAi knockdown of *wrt-1* and, to a lesser degree, *wrt-10* increases the lifespan specifically of mated worms. Mated control,  $15.3 \pm 0.2$  days,  $n = 199$ ; unmated control,  $20.7 \pm 0.5$  days,  $n = 141$ . **h**, Unmated *wrt-1(RNAi)*,  $20.2 \pm 0.4$  days,  $n = 180$ ; mated *wrt-1(RNAi)*,  $18.0 \pm 0.3$  days,  $n = 190$ . Log-rank (Mantel-Cox) test revealed that the lifespan of mated *wrt-1(RNAi)* worms was significantly different from that of mated control worms (\*\*\* $P < 0.001$ ). Two-way ANOVA revealed that mating-induced lifespan decrease of *wrt-1(RNAi)* worms was significantly different from that of control worms ( $P = 0.0016$ ). **i**, Unmated *wrt-10(RNAi)*,  $19.3 \pm 0.4$  days,  $n = 237$ ; mated *wrt-10(RNAi)*,  $16.4 \pm 0.3$  days,  $n = 203$ . Log-rank (Mantel-Cox) test revealed that the lifespan of mated *wrt-10(RNAi)* worms was significantly different from that of mated control worms ( $P = 0.0214$ ). However, two-way ANOVA revealed that mating-induced lifespan decrease of *wrt-10(RNAi)* worms was not significantly different from that of control worms ( $P = 0.6789$ ). **j**, Unmated *Y110A7A.7(RNAi)*,  $18.8 \pm 0.5$  days,  $n = 196$ ; mated *Y110A7A.7(RNAi)*,  $15.8 \pm 0.2$  days,  $n = 233$ . Log-rank (Mantel-Cox) test revealed that the lifespan of mated *Y110A7A.7(RNAi)* worms was not significantly different from that of mated control worms ( $P = 0.0709$ ). Two-way ANOVA revealed that mating-induced lifespan decrease of *Y110A7A.7(RNAi)* worms was not significantly different from that of control worms ( $P = 0.0509$ ). **k**, Expression levels of *wrt-1* and *wrt-10* genes in the germline of *fog-2* and *prde-1* worms (three biological replicates in total, each replicate contains a pool of 200 dissected germlines). Read counts were normalized to the housekeeping gene *rps-4* in each sample. Expression data are presented as mean values  $\pm$  s.d. Expression level of *wrt-1* in unmated *fog-2* germline:  $44 \pm 76$  RPM; mated *fog-2* germline,  $1,732 \pm 1,242$  RPM; unmated *prde-1* germline:  $84 \pm 96$  RPM; mated *prde-1* germline,  $246 \pm 188$  RPM. Expression level of *wrt-10* in unmated *fog-2* germline:  $132 \pm 114$  RPM; mated *fog-2* germline,  $1,118 \pm 62$  RPM; unmated *prde-1* germline,  $189 \pm 137$  RPM; mated *prde-1* germline,  $170 \pm 212$  RPM. **l**, piRNAs targeting *wrt-1* and *wrt-10* target different regions. **m**, Overexpressing *wrt-1* or *wrt-10*-targeting piRNAs is sufficient to prevent mating-induced shrinking. Body size measurements: control (overexpressing 21ur-2671, 21ur-2245, 21ur-1272, 21ur-1114, 21ur-4656 and 21ur-8410) unmated,  $1,361 \pm 84 \mu\text{m}$  ( $n = 20$ ); mated,  $1,073 \pm 109 \mu\text{m}$  ( $n = 28$ ); \*\*\* $P < 0.001$ . *Wrt-1*-targeting piRNAi (overexpressing 21ur-2484 and 21ur-32) unmated,  $1,320 \pm 82 \mu\text{m}$  ( $n = 25$ ); mated,  $1,283 \pm 47 \mu\text{m}$  ( $n = 26$ );  $P = 0.0616$ . *Wrt-10*-targeting piRNAi (overexpressing 21ur-4658 and 21ur-5295) unmated,  $1,312 \pm 97 \mu\text{m}$  ( $n = 25$ ); mated,  $1,284 \pm 102 \mu\text{m}$  ( $n = 22$ );  $P = 0.3427$ .

To test whether any of these 13 genes might be the germline pro-gressing signal, we measured body size postmating after RNAi treatment for each individual gene. Knockdown of three candidates prevented the mated worms from shrinking: two warthog (Hedgehog-like family)

genes, *wrt-1* and *wrt-10*, and an uncharacterized gene, Y110A7A.7 (Fig. 4c, d and Extended Data Fig. 3a, b). Knocking down these three genes specifically in the germline (Fig. 4e), but not in the hypodermis (Fig. 4f) or the intestine (Fig. 4g), was sufficient to protect the mated





hermaphrodites from shrinking, confirming that they are specifically required in the germline to mediate mating-induced shrinking, although *Y110A7A.7* reduction in the germline was less protective of mating-induced shrinking than was *wrt-1* or *wrt-10* knockdown.

In addition to preventing postmating shrinking, inhibiting the bona fide germline pro-aging signal should also increase the lifespan of mated worms. Consistent with this notion, reduction of *wrt-1* provided over 50% protection against mating-induced early death (significant effect determined by both log-rank test and two-way analysis of variance (ANOVA); Fig. 4h). Knocking down *wrt-10* yielded a much milder effect (10% protection, significant by log-rank test,  $P = 0.0214$  but not significant by two-way ANOVA,  $P = 0.6789$ ; Fig. 4i). By contrast, *Y110A7A.7* RNAi did not prevent the worms from mating-induced death (Fig. 4j). Expression of both *wrt-1* and *wrt-10* genes is decreased in a mated *prde-1* mutant compared with mated *fog-2* animals (Fig. 4k). These results suggest that *wrt-1* and, to a much lesser extent, *wrt-10*, may play a critical role in mediating germline pro-aging signaling. Similarly, mating-induced death was partially attenuated in *prde-1* mutants, in which the mating-induced germline upregulation of *wrt-1* and *wrt-10* are abrogated (Extended Data Fig. 4a). The remaining unrescued lifespan decrease is probably caused by the germline-independent mating-induced death mechanisms downstream of seminal fluid transfer<sup>12,14</sup>.

### piRNAs targeting Hh ligands block mating-induced shrinking

To test the specificity of the piRNA pathway in regulating mating-induced shrinking, we overexpressed specific piRNAs in the germline via piRNA-mediated interference<sup>65</sup>. Among 148 significantly downregulated piRNAs in the mated germline, two piRNAs, 21ur-2484 and 21ur-32,

are predicted to target *wrt-1*, whereas another two piRNAs, 21ur-4658 and 21ur-5295, are predicted to target *wrt-10* (piRTarBase; Fig. 4l and Extended Data Fig. 3c). *Wrt-1*- and *wrt-10*-targeting piRNAs were added to the synthetic piRNAi scaffold, while six other non-*wrt* gene targeting piRNAs that are also downregulated in mated germlines were used as the control. Overexpressing piRNAs targeting either *wrt-1* or *wrt-10* was sufficient to prevent mated worms from mating-induced shrinking (Fig. 4m). These data suggest that postmating shrinking—a pro-aging phenotype—is regulated directly by piRNAs that target *wrt-1* and *wrt-10*. Our results suggest that the piRNA pathway and its downstream Hedgehog signaling encode the germline-emanated pro-aging signal.

### Patched receptors mediate mating-induced shrinking and aging

To identify receptors for the Hedgehog ligands secreted from the germline upon mating, we tested the roles of ten Patched receptor homolog genes in shrinking after mating. These genes were chosen because their expression was induced by mating in a germline-dependent manner (Fig. 5a). Knocking down *ptr-6*, *ptr-10* and *ptr-16* prevented mated worms from shrinking (Fig. 5b,c), making them likely candidates to receive the germline-originating signal encoded by *wrt-1* and *wrt-10*. Most Hedgehog signaling receptors, including *ptr-6*, *ptr-10* and *ptr-16*, are predicted to be expressed in the hypodermis (Fig. 5d,e)<sup>66,67</sup>. Using tissue-specific RNAi strains, we found that *ptr-16* in the hypodermis, and *ptr-16* and *ptr-10* in the intestine, were required for mediating mating-induced shrinking (Fig. 5f,g); knockdown in muscle and neurons had no effect, ruling out these tissues as the Hedgehog signal-receiving tissues (Fig. 5h,i). Reducing *ptr-6* and *ptr-16*, but not *ptr-10* or the other

### Fig. 5 | Somatic expression of *ptr-6* and *ptr-16* but not other Patched-related receptor-encoding genes is required for mating-induced death. a,

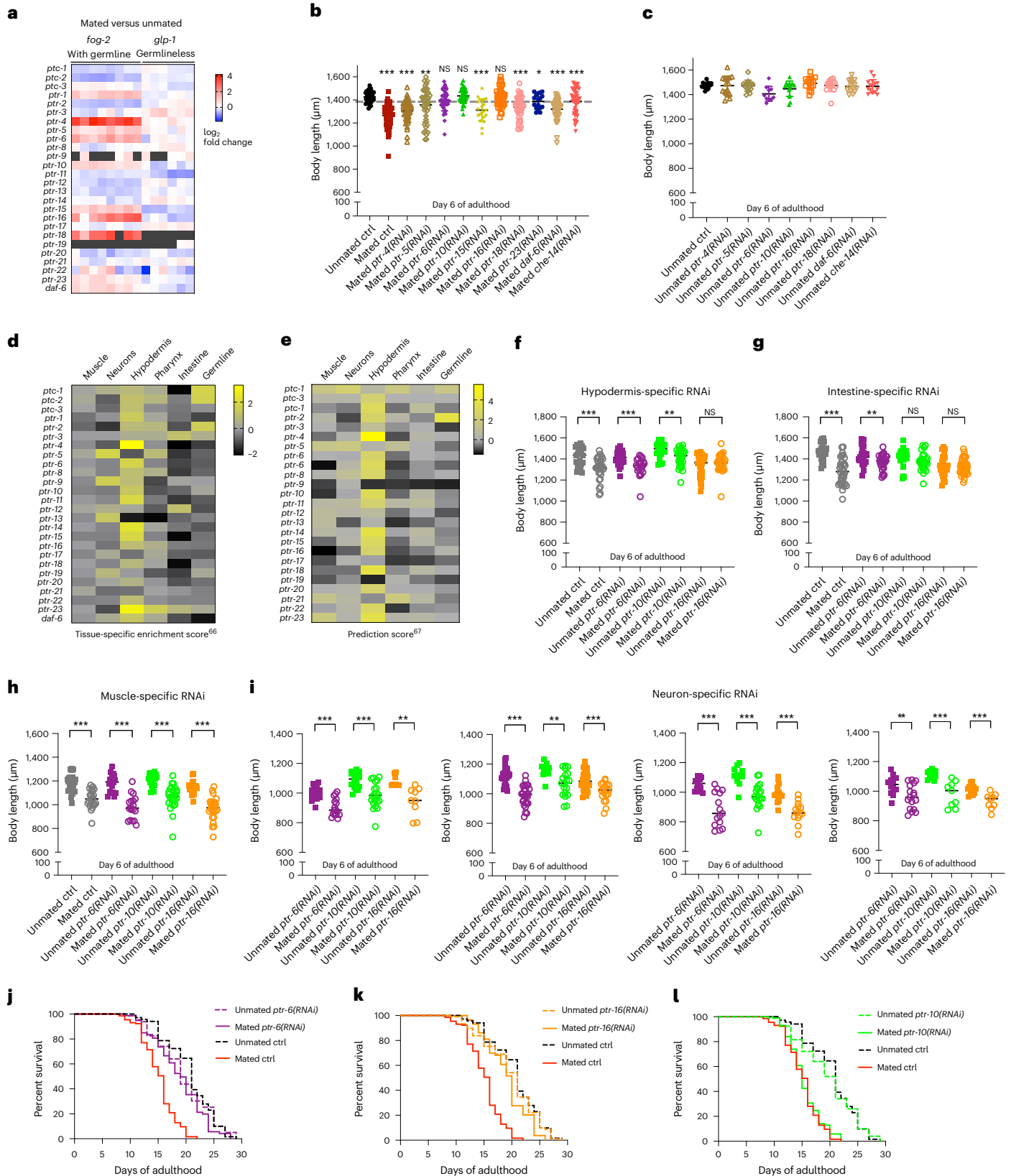
Relative expression (mated versus unmated) of *ptr* homolog genes in worms with a functional germline (*fog-2*) and germlineless worms (*glp-1*). Larger fold changes indicate higher expression after mating. **b**, Body size measurements of mated worms with RNAi treatment of Patched receptor homolog genes. *fog-2(q71)* unmated (control RNAi),  $1,426 \pm 46 \mu\text{m}$  ( $n = 44$ ); mated (control RNAi),  $1,264 \pm 99 \mu\text{m}$  ( $n = 48$ );  $P < 0.001$ ; mated *ptr-4(RNAi)*,  $1,305 \pm 94 \mu\text{m}$  ( $n = 43$ );  $P < 0.001$ ; mated *ptr-5(RNAi)*,  $1,357 \pm 146 \mu\text{m}$  ( $n = 45$ );  $P = 0.0032$ ; mated *ptr-6(RNAi)*,  $1,396 \pm 91 \mu\text{m}$  ( $n = 42$ );  $P = 0.0502$ ; mated *ptr-10(RNAi)*,  $1,436 \pm 65 \mu\text{m}$  ( $n = 34$ );  $P = 0.4623$ ; mated *ptr-15(RNAi)*,  $1,311 \pm 96 \mu\text{m}$  ( $n = 22$ );  $P < 0.001$ ; mated *ptr-16(RNAi)*,  $1,422 \pm 83 \mu\text{m}$  ( $n = 43$ );  $P = 0.7409$ ; mated *ptr-18(RNAi)*,  $1,337 \pm 96 \mu\text{m}$  ( $n = 42$ );  $P < 0.001$ ; mated *ptr-23(RNAi)*,  $1,387 \pm 65 \mu\text{m}$  ( $n = 17$ );  $P = 0.0104$ ; mated *daf-6(RNAi)*,  $1,320 \pm 86 \mu\text{m}$  ( $n = 44$ );  $P < 0.001$ ; mated *che-14(RNAi)*,  $1,388 \pm 112 \mu\text{m}$  ( $n = 44$ );  $P = 0.0394$ . \* $P < 0.05$ , \*\* $P < 0.01$ , \*\*\* $P < 0.001$ . **c**, *ptr* homolog knockdown does not significantly affect the body size of unmated *fog-2* hermaphrodites (unmated control of **b**). Body size measurements: control,  $1,474 \pm 25 \mu\text{m}$  ( $n = 15$ ); *ptr-4*,  $1,473 \pm 78 \mu\text{m}$  ( $n = 15$ ); *ptr-5*,  $1,472 \pm 45 \mu\text{m}$  ( $n = 15$ ); *ptr-6*,  $1,406 \pm 61 \mu\text{m}$  ( $n = 10$ ); *ptr-10*,  $1,448 \pm 63 \mu\text{m}$  ( $n = 15$ ); *ptr-16*,  $1,491 \pm 52 \mu\text{m}$  ( $n = 15$ ); *ptr-18*,  $1,474 \pm 49 \mu\text{m}$  ( $n = 15$ ); *daf-6*,  $1,467 \pm 48 \mu\text{m}$  ( $n = 15$ ) and *che-14*,  $1,468 \pm 53 \mu\text{m}$  ( $n = 15$ ). **d,e**, Tissue-specific expression prediction of Patched receptor homolog genes by the Tissue Expression Predictions for *C. elegans* program, version 1.0 (**d**) and the current version (**e**) (<https://worm.princeton.edu/>). **f**, Hypodermis-specific RNAi strain (DCL569) unmated control,  $1,418 \pm 94 \mu\text{m}$  ( $n = 27$ ); mated control,  $1,309 \pm 104 \mu\text{m}$  ( $n = 32$ );  $P < 0.001$ ; unmated *ptr-6(RNAi)*,  $1,409 \pm 62 \mu\text{m}$  ( $n = 29$ ); mated *ptr-6(RNAi)*,  $1,328 \pm 84 \mu\text{m}$  ( $n = 23$ );  $P < 0.001$ ; unmated *ptr-10(RNAi)*,  $1,483 \pm 78 \mu\text{m}$  ( $n = 21$ ); mated *ptr-10(RNAi)*,  $1,415 \pm 85 \mu\text{m}$  ( $n = 30$ );  $P = 0.0055$ ; unmated *ptr-16(RNAi)*,  $1,340 \pm 102 \mu\text{m}$  ( $n = 34$ ); mated *ptr-16(RNAi)*,  $1,359 \pm 88 \mu\text{m}$  ( $n = 28$ );  $P = 0.4494$ . **g**, Intestine-specific RNAi strain (IG1839) unmated control,  $1,472 \pm 81 \mu\text{m}$  ( $n = 26$ ); mated control,  $1,282 \pm 124 \mu\text{m}$  ( $n = 32$ );  $P < 0.001$ ; unmated *ptr-6(RNAi)*,  $1,433 \pm 93 \mu\text{m}$  ( $n = 24$ ); mated *ptr-6(RNAi)*,  $1,372 \pm 70 \mu\text{m}$  ( $n = 30$ );  $P = 0.0077$ ; unmated *ptr-10(RNAi)*,  $1,411 \pm 85 \mu\text{m}$  ( $n = 26$ ); mated *ptr-10(RNAi)*,  $1,374 \pm 85 \mu\text{m}$  ( $n = 27$ );  $P = 0.1190$ ; unmated *ptr-16(RNAi)*,  $1,328 \pm 103 \mu\text{m}$  ( $n = 24$ ); mated *ptr-16(RNAi)*,  $1,327 \pm 70 \mu\text{m}$  ( $n = 40$ );  $P = 0.9813$ . **h**, Muscle-specific RNAi strain (NR350) unmated control,  $1,184 \pm 77 \mu\text{m}$  ( $n = 23$ ); mated control,  $1,047 \pm 75 \mu\text{m}$  ( $n = 23$ );  $P < 0.001$ ; unmated *ptr-6(RNAi)*,  $1,183 \pm 74 \mu\text{m}$  ( $n = 19$ ); mated *ptr-6(RNAi)*,  $979 \pm 99 \mu\text{m}$  ( $n = 18$ );  $P < 0.001$ ; unmated *ptr-10(RNAi)*,  $1,210 \pm 52 \mu\text{m}$  ( $n = 20$ ); mated *ptr-10(RNAi)*,  $1,064 \pm 99 \mu\text{m}$  ( $n = 27$ );

$P < 0.001$ ; unmated *ptr-16(RNAi)*,  $1,148 \pm 58 \mu\text{m}$  ( $n = 34$ ); mated *ptr-16(RNAi)*,  $966 \pm 99 \mu\text{m}$  ( $n = 24$ );  $P < 0.001$ . **i**, *ptr* genes do not function in the neurons to regulate postmating body size. Four different neuron-specific RNAi strains were used: XE1474, XE1581, XE1582 and XE1375. Body size measurements: XE1474 unmated *ptr-6(RNAi)*,  $1,004 \pm 47 \mu\text{m}$  ( $n = 16$ ); mated *ptr-6(RNAi)*,  $903 \pm 59 \mu\text{m}$  ( $n = 16$ );  $P < 0.001$ ; unmated *ptr-10(RNAi)*,  $1,087 \pm 53 \mu\text{m}$  ( $n = 17$ ); mated *ptr-10(RNAi)*,  $985 \pm 86 \mu\text{m}$  ( $n = 20$ );  $P < 0.001$ ; unmated *ptr-16(RNAi)*,  $1,080 \pm 38 \mu\text{m}$  ( $n = 9$ ); mated *ptr-16(RNAi)*,  $946 \pm 95 \mu\text{m}$  ( $n = 9$ );  $P = 0.0012$ . XE1581 unmated *ptr-6(RNAi)*,  $1,119 \pm 59 \mu\text{m}$  ( $n = 26$ ); mated *ptr-6(RNAi)*,  $987 \pm 70 \mu\text{m}$  ( $n = 27$ );  $P < 0.001$ ; unmated *ptr-10(RNAi)*,  $1,159 \pm 50 \mu\text{m}$  ( $n = 10$ ); mated *ptr-10(RNAi)*,  $1,068 \pm 86 \mu\text{m}$  ( $n = 19$ );  $P = 0.0047$ ; unmated *ptr-16(RNAi)*,  $1,088 \pm 67 \mu\text{m}$  ( $n = 23$ ); mated *ptr-16(RNAi)*,  $1,013 \pm 62 \mu\text{m}$  ( $n = 19$ );  $P < 0.001$ . XE1582 unmated *ptr-6(RNAi)*,  $1,055 \pm 41 \mu\text{m}$  ( $n = 13$ ); mated *ptr-6(RNAi)*,  $882 \pm 113 \mu\text{m}$  ( $n = 15$ );  $P < 0.001$ ; unmated *ptr-10(RNAi)*,  $1,111 \pm 65 \mu\text{m}$  ( $n = 11$ ); mated *ptr-10(RNAi)*,  $975 \pm 86 \mu\text{m}$  ( $n = 20$ );  $P < 0.001$ ; unmated *ptr-16(RNAi)*,  $995 \pm 61 \mu\text{m}$  ( $n = 14$ ); mated *ptr-16(RNAi)*,  $865 \pm 72 \mu\text{m}$  ( $n = 13$ );  $P < 0.001$ . XE1375 unmated *ptr-6(RNAi)*,  $1,041 \pm 63 \mu\text{m}$  ( $n = 12$ ); mated *ptr-6(RNAi)*,  $961 \pm 82 \mu\text{m}$  ( $n = 17$ );  $P = 0.0096$ ; unmated *ptr-10(RNAi)*,  $1,114 \pm 26 \mu\text{m}$  ( $n = 13$ ); mated *ptr-10(RNAi)*,  $980 \pm 85 \mu\text{m}$  ( $n = 9$ );  $P < 0.001$ ; unmated *ptr-16(RNAi)*,  $1,015 \pm 33 \mu\text{m}$  ( $n = 11$ ); mated *ptr-16(RNAi)*,  $932 \pm 52 \mu\text{m}$  ( $n = 9$ );  $P < 0.001$ . \*\* $P < 0.01$ , \*\*\* $P < 0.001$ . **j–l**, RNAi knockdown of *ptr-6* and *ptr-16* increases the lifespan of mated worms. Mated control,  $15.1 \pm 0.3$  days,  $n = 257$ ; unmated control,  $20.6 \pm 0.5$  days,  $n = 99$ . **j**, Unmated *ptr-6(RNAi)*,  $19.6 \pm 0.6$  days,  $n = 91$ ; mated *ptr-6(RNAi)*,  $18.8 \pm 0.5$  days,  $n = 114$ . Log-rank (Mantel–Cox) test revealed that the lifespan of mated *ptr-6(RNAi)* worms was significantly different from that of mated control worms ( $P < 0.001$ ). Two-way ANOVA revealed that mating-induced lifespan decrease of *ptr-6(RNAi)* worms was significantly different from that of control worms ( $P = 0.0037$ ). **k**, Unmated *ptr-16(RNAi)*,  $19.8 \pm 0.5$  days,  $n = 105$ ; mated *ptr-16(RNAi)*,  $19.1 \pm 0.5$  days,  $n = 120$ . Log-rank (Mantel–Cox) test revealed that the lifespan of mated *ptr-16(RNAi)* worms was significantly different from that of mated control worms ( $P = 0.0214$ ). Two-way ANOVA revealed that mating-induced lifespan decrease of *ptr-16(RNAi)* worms was significantly different from that of control worms ( $P = 0.0003$ ). **l**, Unmated *ptr-10(RNAi)*,  $19.7 \pm 0.7$  days,  $n = 100$ ; mated *ptr-10(RNAi)*,  $15.5 \pm 0.3$  days,  $n = 120$ . Log-rank (Mantel–Cox) test revealed that the lifespan of mated *ptr-10(RNAi)* worms was not significantly different from that of mated control worms ( $P = 0.0709$ ). Two-way ANOVA revealed that mating-induced lifespan decrease of *ptr-10(RNAi)* worms was not significantly different from that of control worms ( $P = 0.5749$ ).

Patched-related receptor genes, rescued mating-induced early death (Fig. 5j–l). *Ptr-6* and *ptr-16* RNAi yielded a similar or greater degree of protection compared with *wrt-1* RNAi in mated worms (Fig. 6a). Moreover, PTR-16 is predicted to interact with WRT-1 according to the STRING database (Fig. 6b), which integrates all publicly available sources of protein–protein interaction information<sup>68</sup>. To test this potential interaction, we performed yeast two-hybrid assays; a modest interaction

between WRT-1 and PTR-16 was observed (Fig. 6c,d), suggesting that PTR-16 is most probably the receptor that receives the pro-aging Hedgehog WRT-1 signal from the germline upon mating.

Finally, we wondered whether there is any generational penalty for eliminating mating-induced shrinking and death, as these processes are deleterious to the mother. While *wrt-1*, *wrt-10*, *ptr-6* and *ptr-16* knock-down all produce unmated brood sizes similar to those of wildtype



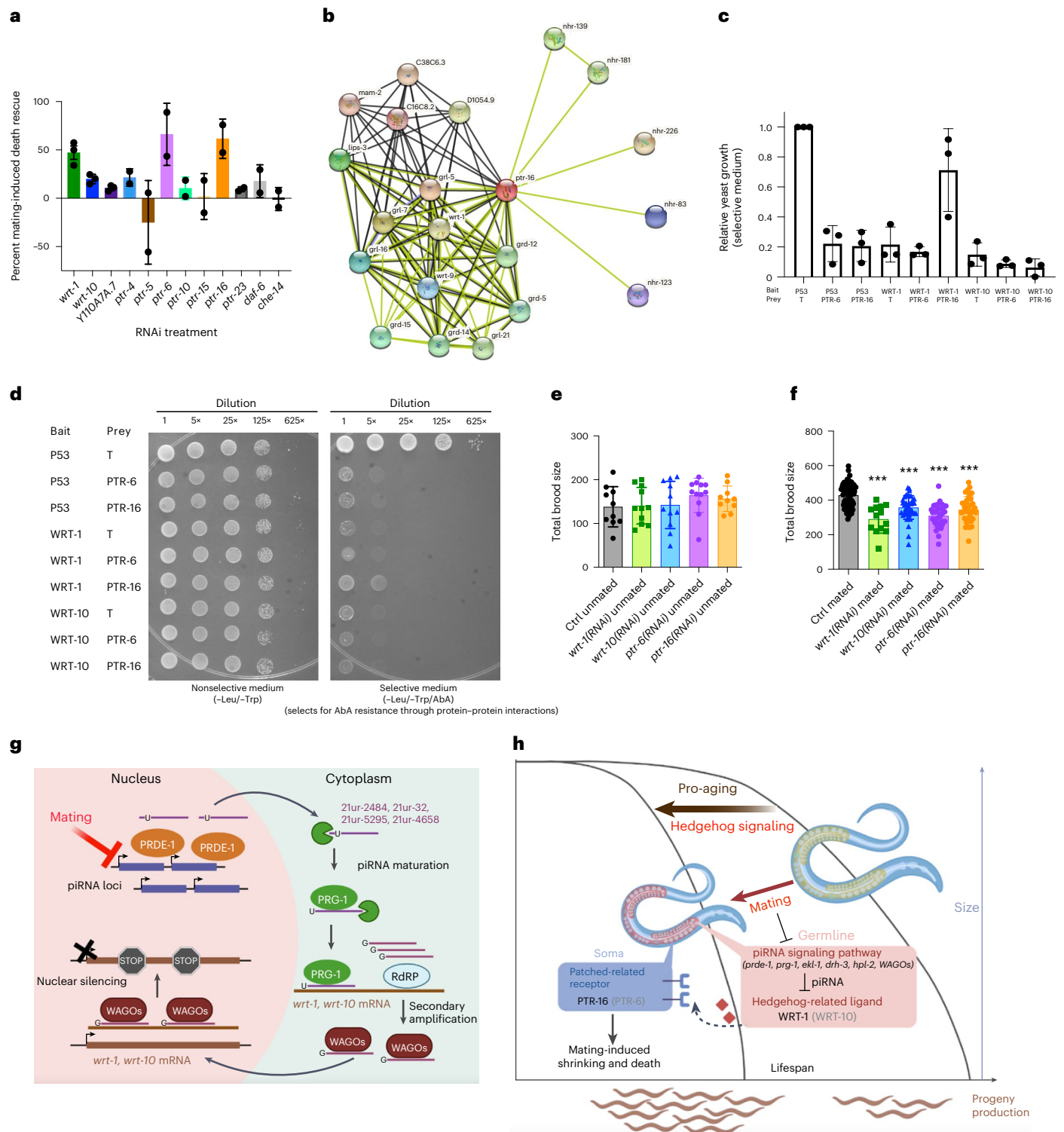


(Fig. 6e), knockdown of Hedgehog signaling components in mated worms led to a 20–30% reduction in brood size (Fig. 6f;  $P < 0.001$ ). Therefore, while inhibiting germline piRNA-mediated Hedgehog signaling is beneficial to the mothers, as it prevents mated worms from shrinking and largely rescues mating-induced death, such benefits do not come without a cost to progeny. Signaling from the mated germline, while deleterious to the mother’s soma and ultimately leading to her death, may be an unavoidable cost of activation of the germline upon mating that is necessary for sufficient nutrient provisioning to progeny.

## Discussion

In animals across taxa, germline hyperactivity leads to accelerated aging<sup>14</sup>; however, the underlying mechanisms are poorly understood. Here we found that mating-induced piRNA downregulation in the germline releases suppression of the Hedgehog signaling pathway, which in turn leads to body size and lifespan decrease in mated worms (Fig. 6g,h). Our results suggest that piRNA-regulated Hedgehog signaling encodes the previously unknown and long-sought germline-to-soma pro-aging signal<sup>7</sup>.

**Fig. 6 | Hedgehog signaling encodes the germline-to-soma aging signal in mated hermaphrodites.** **a**, Summary of the mating-induced death rescue effect of RNAi knockdown of individual Hedgehog signaling components. Each black dot represents one biological replicate of the lifespan assay. Data are presented as mean values of rescue effect  $\pm$  s.d. (error bars). Three replicates of lifespan assays were performed for worms treated with *wrt-1*, *wrt-10* and *Y110A7A.7* RNAi. Two replicates of lifespan assays were performed for worms treated with *ptr-4*, *ptr-5*, *ptr-6*, *ptr-10*, *ptr-15*, *ptr-16*, *ptr-23*, *daf-6* and *che-14* RNAi. **b**, PTR-16 interaction network predicted by STRING. **c**, Relative yeast cell growth on selective medium (quantified from the fivefold dilution spots on yeast two-hybrid assay plates, see **d** and Methods for details). Data are presented as relative growth  $\pm$  s.d. Three independent replicates of yeast two-hybrid assay were performed. **d**, Representative pictures of yeast two-hybrid assay. A dominant mutant version of the AURI gene that encodes the enzyme inositol phosphoryl ceramide synthase is expressed in the Y2HGold yeast strain in response to positive interaction between the bait and prey, conferring strong resistance to the otherwise highly toxic drug AbA. The final concentration of AbA on plates was 200 ng ml<sup>-1</sup>. Single colonies of each type were inoculated and allowed to grow overnight at 30 °C to reach stationary phase (OD > 1.5). From the culture,

20  $\mu$ l of undiluted culture and 5 $\times$ , 25 $\times$ , 125 $\times$  and 625 $\times$  dilutions were spotted on the assay plates. Plates were imaged after incubating for 4 days at 30 °C. Quantification of yeast growth of the fivefold dilution spots is shown in **c**. Growth on selective medium was normalized to growth on nonselective medium first before comparing with the positive control spot (P53-T); Methods). **e**, Inhibiting Hedgehog signaling by RNAi does not affect the unmated (self-fertilized) brood size of the wildtype N2 hermaphrodites. N2 control unmated, 138  $\pm$  46,  $n$  = 10; *wrt-1*(RNAi) unmated, 141  $\pm$  42,  $n$  = 11; *wrt-10*(RNAi) unmated, 142  $\pm$  54,  $n$  = 11; *ptr-6*(RNAi) unmated, 164  $\pm$  39,  $n$  = 12; *ptr-16*(RNAi) unmated, 156  $\pm$  29,  $n$  = 10. Data are presented as total brood size  $\pm$  s.d. **f**, Inhibiting Hedgehog signaling by RNAi in mated N2 hermaphrodites leads to significantly reduced total mated brood size. Control mated, 429  $\pm$  67,  $n$  = 65; *wrt-1*(RNAi) mated, 290  $\pm$  81,  $n$  = 13; *wrt-10*(RNAi) mated, 358  $\pm$  68,  $n$  = 41; *ptr-6*(RNAi) mated, 310  $\pm$  65,  $n$  = 33; *ptr-16*(RNAi) mated, 345  $\pm$  76,  $n$  = 38. Data are presented as total brood size  $\pm$  s.d. \*\*\* $P$  < 0.001: two-tailed unpaired  $t$ -test was used for total mated brood size comparison (all were compared with that of control mated worms). **g**, Model of the role of mating in piRNA-mediated regulation of *wrt-1* and *wrt-10* expression. **h**, Model of piRNA-mediated Hedgehog signaling as the germline-to-soma pro-aging signal in mated hermaphrodites.

The Hedgehog signaling pathway is a key regulator of animal development<sup>69</sup>; our study provides evidence for an additional critical role in adult postmating lifespan regulation in *C. elegans*, distinct from its role in developmental growth processes. Hedgehog signaling also participates in adult soma-to-germline communication: overexpression of hypodermal *wrt-10* delays reproductive decline and improves germline health<sup>70</sup>. Therefore, *wrt-10* could function as a feed-forward loop in mated worms, achieving sustained germline hyperactivity at the cost of exacerbated somatic collapse (that is, shrinking). Our results suggest that there is likely a trade-off between somatic integrity and progeny production in mated animals, as demonstrated by the reduced mated brood size of animals with reduced Hedgehog signaling (Fig. 6h).

The involvement of Hedgehog signaling in lifespan regulation is not limited to worms. Altered Hedgehog signaling reduces survival of *Drosophila* larvae under starvation<sup>71</sup>, impaired Hedgehog signaling in glia affects the lifespan of adult *Drosophila*<sup>72</sup> and the Hedgehog pathway inhibitor saridegib dramatically increases lifespan by fourfold in a mouse medulloblastoma model<sup>73</sup>. Therefore, Hedgehog signaling seems to have an evolutionarily conserved role in lifespan regulation beyond its well-established function in development.

Our results unveil a new function for the piRNA pathway in transcriptional regulation, an underappreciated aspect of piRNA biology compared with its better-studied role in germline repression of transposable elements (TE)<sup>74</sup>. TE-independent piRNA functions in endogenous mRNA regulation of developmental processes include embryonic patterning, germ cell specification and stem cell biology<sup>75</sup>. Our results expand the roles of piRNA pathways in the regulation of gene expression to adult functions<sup>59,76,77</sup>. Here, we describe piRNA-mediated regulation of a known signaling pathway in the adult germline (Fig. 6g,h). These results also highlight the fact that piRNA expression is regulated and tunable by mating status.

Mating-induced germline-to-soma piRNA-mediated Hedgehog signaling elegantly coordinates germline function and somatic aging. In an unmated female with low or no germline proliferation, the priority of the germline is to maintain its integrity until mating occurs, while avoiding unnecessary proliferation or differentiation of the germ cells. piRNAs contribute to this process by suppressing errant TE expression and developmental programs, including those regulated by Hedgehog signaling. By contrast, upon mating, the germline switches to progeny production mode, and the previous suppression of Hedgehog signaling by piRNAs is released to allow rapid germline stem cell proliferation and further differentiation (Fig. 6g). As Hedgehog ligands are secreted, activated Hedgehog signaling may be co-opted as a germline-to-soma signal to coordinate the somatic responses to elevated germline activity. Postmating shrinking correlates with the reallocation of somatic

resources to the germline<sup>12,13,78</sup> and the reduction in energy devoted to somatic integrity maintenance, reflecting the direct cost of germline hyperactivity and substantially increased progeny production. Signaling from the mated germline, while deleterious to the mother's soma and ultimately leading to her death, may be an unavoidable cost of activation of the germline upon mating that is necessary for sufficient nutrient provisioning to progeny. Our study reveals a mechanism that can efficiently convey germline status to the soma in adulthood, allowing the animals to better organize the balance between reproduction and somatic maintenance, optimizing reproductive fitness.

Of the three mating-related killing mechanisms—male pheromone, seminal fluid, and sperm activation of germline proliferation—the last has the highest chance of being evolutionarily conserved. Male pheromone-induced killing kills hermaphrodites only at nonphysiologically high concentrations, and kills males specifically but only in androdioecious species<sup>13</sup>. Seminal fluid kills the mother by turning off her IIS/FOXO protective pathway<sup>12,13</sup>, which is unnecessary for successful reproduction. By contrast, germline activation upon mating is the most likely to be both necessary and shared with other animals, as germline activity correlates with shorter lifespan in worms, flies, mice, and possibly humans<sup>7-12,14</sup>. Because germline proliferation may be induced by mating in other organisms, and piRNAs are ubiquitous in animal germlines, it will be interesting to see whether mating-induced piRNA regulation of signaling from germline to somatic tissues is conserved.

## Methods

### Strains

*C. elegans* strains used in the study were as follows:

Strains	Genotype	Source
N2	Wildtype	CGC
CB4108	<i>fog-2(q71) V</i>	CGC
CB4037	<i>glp-1(e2141) III</i>	CGC
HC196	<i>sid-1(qt9) V</i>	CGC
CS1	<i>sma-9(wk55) X</i>	CGC
YY470	<i>dcr-1(mg375) III</i>	CGC
SX922	<i>prg-1(n4357) I</i>	CGC
SX2499	<i>prde-1(mj207) V</i>	CGC
VC3150	<i>ekl-1(ok1197) I/hT2 [bli-4(e937) let-?(q782) qls48] (I;III)</i>	CGC
WM140	<i>drh-3(tm1217) I/hT2 [bli-4(e937) let-?(q782) qls48] (I;III); him-8(e1489) IV</i>	CGC
RB995	<i>hpl-2(ok916) III</i>	CGC

WM191	MAGO12 mutant. Full genotype: <i>sago-2(tm894)</i> <i>ppw-1(tm914)</i> <i>ppw-2(tm1120)</i> <i>wago-2(tm2686)</i> <i>wago-1(tm1414)</i> I; <i>wago-1(tm1127)</i> <i>wago-5(tm1113)</i> <i>wago-4(tm1019)</i> II; <i>hrde-1(tm1200)</i> <i>sago-1(tm1195)</i> III; <i>wago-10(tm1186)</i> V; <i>nrrde-3(tm1116)</i> X.	CGC
JH3225	<i>meg-3(tm4259)</i> <i>meg-4(ax2026)</i> X	CGC
JH3229	<i>meg-1(vr10)</i> <i>meg-3(tm4259)</i> X.	CGC
CQ655	<i>prg-1(n4357)</i> I; <i>unc-119(ed3)</i> III; <i>vrls79[Ppie-1::GFP::prg-1+unc-119(+)]</i>	Murphy laboratory
CQ479	<i>rde-1(ne219)</i> ; <i>wqEx50[Pdpy-7::GFP; pY37A1B.5::GFP; Pdpy-7::rde-1::unc-54 3'UTR; PY37A1B.5::rde-1::unc-54 3'UTR]</i>	Murphy laboratory
DCL569	<i>mkcSi13</i> II; <i>rde-1(mkc36)</i> V	CGC
IG1839	<i>frSi17</i> II; <i>frls7</i> IV; <i>rde-1(ne300)</i> V	CGC
NR350	<i>rde-1(ne219)</i> V; <i>kzls20</i>	CGC
XE1474	<i>wpSi6</i> II; <i>eri-1(mg366)</i> IV; <i>rde-1(ne219)</i> V; <i>lin-15B(n744)</i> X.	CGC
XE1581	<i>wpSi10</i> II; <i>eri-1(mg366)</i> IV; <i>rde-1(ne219)</i> V; <i>lin-15B(n744)</i> X	CGC
XE1582	<i>wpSi11</i> II; <i>eri-1(mg366)</i> IV; <i>rde-1(ne219)</i> V; <i>lin-15B(n744)</i> X	CGC
AA278	<i>dhls59</i> [Topo::daf-9::GFP+ <i>lin-15(+)</i> ]	CGC
XE1375	<i>wpls36</i> I; <i>wpSi1</i> II; <i>eri-1(mg366)</i> IV; <i>rde-1(ne219)</i> V; <i>lin-15B(n744)</i> X	CGC
WM300	<i>alg-4(ok1041)</i> III; <i>alg-3(tm1155)</i> IV	CGC
YY968	<i>znfx-1(gg544[3xflag::gfp::znfx-1])</i> II; <i>pgl-1(gg547[pgl-1::3xflag::tagRFP])</i> IV	CGC

### Germline dissection

Germline dissection was modified from a previous publication<sup>79</sup>. Worms were transferred to iced M9 buffer for dissection. Heads or tails were removed with 26G needles, allowing the distal portion of the germline to pop out of the worm. Glass capillaries pulled with an opening just large enough to fit the end of the germline were used to detach them rapidly at the ventral-to-distal bend. Dissected distal germlines were transferred immediately into 1.5 ml Eppendorf tubes filled with 500  $\mu$ l Trizol. About 200 germlines were collected for each biological replicate.

### RNA isolation and library preparation

Tubes containing dissected germlines (immersed in Trizol) were put in an Eppendorf MixMate Vortex Mixer at 800 r.p.m. and 65 °C for 1 h before the isolation process. Total RNA was extracted from Trizol using the mirVana miRNA isolation kit (ThermoFisher). mRNA libraries for directional RNA-seq were prepared using the SMARTer Apollo System and were sequenced (150-nt single-end) on the Illumina NovaSeq platform. RNA samples for small RNA-seq were treated with 5' polyphosphatase (Lucigen) and prepared using the SMARTer Apollo system with modifications for small RNA library preparation. Small RNA-containing libraries were Blue Pippin size selected (15–30 nt insert size) before 75-nt single-end sequencing.

### Transcriptome data analysis

**RNA-seq.** FASTQC was used to assess read quality scores. Universal adapter sequences were trimmed from small RNA library sequences using Cutadapt. Reads were mapped to the *C. elegans* genome (UCSC February 2013, ce11/ws245) using Bowtie. Count matrices were generated using featureCounts. Data were normalized with a variance-stabilizing transformation (DESeq2). DESeq2 was used for differential expression analysis. Genes at  $P_{adj} < 0.05$  were considered significantly differentially expressed. PCA was carried out using the R method (prcomp). Heatmaps were generated in R using normalized read counts (variance-stabilizing transformation). Tissue enrichment and

gene ontology (GO) term enrichment analysis were performed using wormbase enrichment analysis (<https://wormbase.org/tools/enrichment/tea/tea.cgi>) for significantly differentially-expressed genes. Predicted targets of piRNAs were retrieved from piRTarBase (<http://cosbi6.ee.ncku.edu.tw/piRTarBase/>) using the default 'relaxed' piRNA targeting setting, see Supplementary Data 2 for the full list. Sequences were deposited at NCBI BioProject PRJNA892981.

**Microarrays.** Microarray data of mated and unmated *glp-1(e2141)* was retrieved from a previous publication<sup>34</sup>. Microarray data of mated and unmated *fog-2(q71)* was retrieved from a previous publication<sup>61</sup>. Hermaphrodites were mated on Day 1 of adulthood for 24 h in a 2:1 male:hermaphrodite ratio. About 200 hermaphrodites were collected on Day 2/3 of adulthood for each biological replicate. RNA was extracted by the heat vortexing method. Two-color Agilent microarrays were used for expression analysis. Significantly differentially-expressed gene sets were identified using significance analysis of microarrays (SAM)<sup>80</sup>. One-class SAM was performed to identify genes that are significantly differentially expressed after mating. The lists were then compared with significantly upregulated genes in dissected germline (RNA-seq).

### Lifespan

NGM plates (60 mm) plates were used to set up group mating. Each 60 mm NGM plate was seeded with OP50 to make a bacterial lawn of around 3 cm in diameter 2 days before mating. All lifespan assays were performed at room temperature (20–21 °C). About 50 hermaphrodites and 100 young (Day 1–2 of adulthood) males were transferred onto the plate. Then, 24–48 h later, the hermaphrodites were transferred onto newly seeded 60 mm NGM plates in the absence of males for lifespan assays. No 5-fluoro-2'-deoxyuridine was added to the plates. We confirmed successful mating for all worms by checking their progeny. With successful mating, about half of the progeny are male. For the only two sterile strains used in this study, *ekl-1* and *drh-3* homozygous mutants, we confirmed successful mating empirically by observing the decrease in darkness of mated sterile worms under normal light, which indicates mating-induced fat loss. About 25 synchronized Day 1 hermaphrodites were transferred onto each plate. The hermaphrodites were transferred daily onto new seeded plates in the first week of the lifespan assay. Afterward, they were transferred once every 2 days. When RNAi was used in lifespan assay, RNAi treatment always started from eggs for all the experiments in this study. Kaplan–Meier analysis with log-rank (Mantel–Cox) method was performed to compare the lifespans of different groups. 'Bagged' worms were censored on the day of the event.

### Body size measurements

Mating set up was the same as described in Lifespan. We confirmed successful mating for all the worms by checking their progeny. With successful mating, about half of the progeny are male. For the only two sterile strains used in this study, *ekl-1* and *drh-3* homozygous mutants, we confirmed the successful mating empirically by observing the decrease in darkness of mated sterile worms under normal light, which indicates mating-induced fat loss. Images of live hermaphrodites on 60 mm plates were taken on Day 6/7 of adulthood with a Nikon SMZ1500 microscope. When RNAi was used, RNAi treatment always started from eggs for all the experiments. ImageJ was used to analyze the body size of the worms. The middle line of each worm was delineated using the segmented line tool and the total length was documented as the body length of the worm. A *t*-test was performed to compare the body size differences between groups of worms in the same day.

### Brood size

Individual hermaphrodites after mating were transferred onto 3 cm NGM plates seeded with 25 ml OP50 and moved to fresh plates daily

until reproduction ceased. The old plates were left at 20 °C for 2 days to allow the offspring to grow into adults, which were counted manually for daily production and total brood size. Between 10 and 25 plates of individual worms of each genotype per treatment were counted to account for individual variation.

### P granule imaging and quantification

mCherry-tagged fluorescent PGL-1 was visualized in living nematodes (YY968) by mounting young adult animals on 2% agarose pads with M9 buffer with 20 mM levamisole. Fluorescent images were captured using a Nikon Ti microscope with a ×100 objective. Images were processed and quantified in ImageJ. The quantification of germline granule fluorescence was performed using ImageJ. For every image, a region of interest (ROI) with a clear focus of P granules was selected manually. The area of the whole ROI was kept the same for all images. The number of puncta within the ROI was measured blindly for each germline and image. The densities of germline P granules were calculated as: the number of puncta within the ROI per the area of the whole ROI. Densities of germline granules were determined for 50–60 ROIs, and the mean and s.d. were calculated using GraphPad Prism. A *t*-test was performed to compare the P granule density differences between mated and unmated germlines.

### Germline piRNA overexpression

We modified recently developed piRNAi<sup>65</sup> to overexpress endogenous piRNAs. The scaffold information was obtained from the website <https://www.wormbuilder.org/piRNAi/>. Cluster was generated using simple search option with the default setting (targeted gene: *wrt-1* or *wrt-10*). Synthetic piRNAs were replaced by endogenous piRNAs as indicated by the text and figure legends. The sequences (about 1.5 kb) were synthesized by Twist Bioscience. The injection mix consisted of 20 ng μl<sup>-1</sup> synthetic dsDNA piRNA overexpression cluster with adapters that were not further purified (Twist Bioscience), 2 ng μl<sup>-1</sup> coinjection marker (Pmyo2::mCherry::unc-54 3' UTR), and 1 kb DNA ladder to a final total DNA concentration of 100 ng μl<sup>-1</sup>. F1 progeny with red pharynx were selected from injected animals. Synchronized F2 progeny from positive transgenic F1 worms were used in mating and body size measurement assays.

The sequences of piRNA overexpression clusters used in this study are as follows:

piRNA overexpression cluster targeting *wrt-1* (uppercase: piRNAs)

cgcgcttgacgcgctagtagcaactaacataaaaaaggtgaaacattgagcaggatacatagaaaaacaatacttcaattcattttcaattacaactcctgaaatgtttcactgttctataagaaaaacattgaaacaaaatattaagtTAGAACTTCATCTTTAGAACActaattttgattgtttgaaatcgaattgcaaatccaataaaaaatcattttctgataatagacagttcctatcgtaatttttattatctatcgagttagaaattgcaacgaagataatgtcttcaaaactgaaaattgaaaatgtttttatgagcaggtgctgacggattgccgaactcaaaatgaaattttatagttttgaaacagtaagaaaactgtgaattactgaaactggttctttttaaagtaacctacttcaaatctacttcaaaatataatgtttcaaatcaactgtgtgaaagttggcgcccagttgactgtagagcttcaatgttgataagattataacacagtgaaacaggttaatgtttgttgcaaaatcggaactctacattcatatggttttaattacaggtttttataaaaaatgtgtgatggatatttttcagacctacataactgcaaaccttcaacaatgtgaagctactctgtttcactcaaccattcattcaattggaaaaaaatcaaaagaaatgtgaaaaatcttctgtttcaacattatgacaaaaatgttatgatttaataaaaaaatTGCATAACGTAGAACATCATcttctgttttctagaaggttttc-cggaacgcgtaattggttttatcacaatcgaaacaaaacaaaattttttaattttctt-gctagttttgtagttgaaaattcactataatcatgaataagtgagctgcccaagtaacaa-gaaaattggcagcggccgacaactaccgggtgcccagttatcagtgaggatctacaaggctaacgtctatctaatgtgatgtacacggttttcatttaaaacaaatgaaacagaaatgactacatttcaaatgtctattttgctgtgtttatgtccaccaacaat-tagccttgcaacttagtaaacctcaatgaattcctccagccacatatgtaaacggtgtatacatgcagaaaacggtttttggtttaattgggaactttgcaaaatcttaagctgtccattcagttgggtgatcgatt

piRNA overexpression cluster targeting *wrt-10* (uppercase: piRNAs)

cgcgcttgacgcgctagtagcaactaacataaaaaaggtgaaacattgagcaggatacatagaaaaacaatacttcaattcattttcaattacaactcctgaaatgtttcactgtgttctataagaaaaacattgaaacaaaatattaagtTAAATGAAAAGCTGGCTATG-Gctaattttgattttgaaatcgaattgcaaatccaataaaaaatcattttctgataatagacagttcctatcgtaattttatatactatcgagttagaaattgcaacgaagataatgtcttcaaaactgaaaatgtgaaaatgtttttatgagcaggtgctgacggattgccagaactcaaaatgaaaatttttagttttgtgaaacagtaagaaaacttgttaattactgttaaac-tgttctttttaaagtaacctacttcaaatctacttcaaaaaattataatgtttcaaatcaat-aactgtgtgaaagttggcgcccagttgactgtagagcttcaatgttgataagatttataaca-cagtgaaacaggtatagttgtttgtgcaaaaatcggaactctacatttcatatggtttt-taattacaggtttgtttataaaaaatgtgtgatggatatttttcagacctacataactc-gcaaacctcaacaatgtgaaagctactctgtttcactcaaccattcattcaattggga-aaaaatcaaaagaaatgtgaaaatcttctgtttcaacattatgacaaaaatgttatgatt-taataaaaaaatTGAATAGCGTAAACAAAAGAttctgtttttctagaaggtttttc-cggaacgcgtaattggttttatcacaatcgaaacaaaacaaaattttttaattttctt-gctagttttgtagttgaaaattcactataatcatgaataagtgagctgcccaagtaacaa-gaaaattggcagcggccgacaactaccgggtgcccagttatcagtgaggatctaca-ggtaactcgcttatctaatgtgatgtacacggttttcatttaaaacaaatgaaacagaaat-gactacatttcaaatgtctattttgctgtgtttatgtccaccaacaatgagataatgtgt-tagccttgcaacttagtaaacctcaatgaattcctccagccacatatgtaaacggtgt-tatacatgcagaaaacggtttttggtttaattgggaactttgacaaattgttcgaaaatct-taagctgtccattcagttgggtgatcgatt

piRNA overexpression cluster control (uppercase: piRNAs)

cgcgcttgacgcgctagtagcaactaacataaaaaaggtgaaacattgagcaggatacatagaaaaacaatacttcaattcattttcaattacaactcctgaaatgtttcactgtgttctataagaaaaacattgaaacaaaatattaagtTAGAAACTGATCTTCAAAA-GTctaattttgattttgaaatcgaattgaaatccaataaaaaatcattttctgataatagacagttcctatcgtaattttatatactatcgagttagaaattgcaacgaagataatgtcttcaaaactgaaaatgtgaaaatgttACTTTCCATAACGTCGACAAAattggca-gaactcaaaatgaaatttatagttttgtgaaacagtaagaaaactgtgaattactgt-taaactgttctttttaaagtaacctacttcaaatctacttcaaaatataatgtttcaaat-tacataactgtgtAATTCGGGAGTCTAATTTAactgtagagcttcaatgttgataa-gatttataacacagtgaaacaggttaatgtttgtttgcaaaatcggaactctacattcatt-atggttttttaacaggtttgtttataaaaaatgtgtgatggatatttttcagacctacataaactgcaaaccttcaacaatgtgaaagctactctgtttcactcaaccattcattcaattgg-aaaaaaatcaaaagaaatgtgaaaatcttctgtttcaacattatgacaaaaatgttatgatt-taataaaaaaatGAAAATTTGCTGAACACCTTtctgtttttctagaaggtttttc-cggaacgcgtaattggttttatcacaatcgaaacaaaacaaaattttttaattttctt-gctagttttgtagttgaaaattcactataatcatgaataagtgagctgcccaagtaacaa-gaaaattggcagcggccgacaactaccgggtgcccagttatcagtgagggaGATC-GAGGCTTAATGAACGGAatctaattgtgatgtacacggttttcatttaaaacaaatt-gaaacagaaatgactacatttcaaatgtctattttgctgtgtttatgtccaccaacaat-TAAAAGTGGCTCCGAGCTAGGtcaactagtaaacctcaatgaattcctc-cagccacatatgtaaacggtgtatacatgcagaaaacggtttttggtttaattgggaacttt-gacaaattgttcgaaaatcttaagctgtccattcagttgggtgatcgatt

### Adapter sequences

Twist Primer Set 2 Fw: 5'-CAATCCGCCCTCACTACAACCG-3'

Twist Primer Set 2 Rev: 5'-TCCCTCATCGACGCCAGAGTAG-3'

### Yeast two-hybrid assay

Yeast two-hybrid assay was performed using Takara Matchmaker Gold Yeast Two-Hybrid System (catalog no. 630489). WRT-1 and WRT-10 cDNA were cloned in frame into the bait construct pGBKT7, whereas PTR-6 and PTR-16 cDNA were cloned in frame into the prey construct pGADT7. pGBKT7-53, which encodes the Gal4 DNA-BD fused with murine p53, and pGADT7-7, which encodes the Gal4 AD fused with SV40 large T-antigen, were used as positive interaction controls in the assay. The bait constructs and the prey constructs were cotransformed into Y2HGold yeast strain in various combinations to test potential interaction. A dominant mutant version of the AUR1 gene that encodes the enzyme inositol phosphoryl ceramide synthase is expressed in Y2HGold Yeast strain in response to positive interaction between the bait and prey, conferring strong resistance to the otherwise highly toxic drug Aureobasidin A (AbA). The final

concentration of ABA used in the assay was 200 ng ml<sup>-1</sup>. Single colonies of each type were inoculated and allowed to grow overnight at 30 °C to reach stationary phase (OD > 1.5). From the culture, 20 µl of undiluted, 5×, 25×, 125× and 625× dilutions were spotted on the assay plates. Plates were imaged after incubating for 4 days at 30 °C. Quantification of yeast growth was performed according to the published protocol<sup>81</sup>.

### Tissue expression prediction

Tissue enrichment prediction analyses for ptr genes were performed using two methods: (1) the Tissue Expression Predictions for *C. elegans* program, v.1.0 (<http://worm-tissue.princeton.edu/search/multi>). The tissue-specific enrichment scores were used to generate the heatmap in Fig. 5d. Genes bulk query for their predicted tissue expression (<https://worm.princeton.edu/>). The prediction scores of principal tissues were used to generate the heatmap in Fig. 5e.

### Intestinal barrier function assay (Smurf assay)

The intestinal barrier function assay (Smurf assay) was performed according to the published protocol<sup>82</sup> with a few modifications. Briefly, synchronized Day 1 worms were set up for mating. About 50 worms were removed from the mating plate or the control plate 48 h later, and suspended overnight in liquid cultures of OP50 bacteria mixed with blue dye (bromophenol blue, 0.4 g 100 ml<sup>-1</sup> M9). Animals were then washed three times with M9 buffer before imaging using Nikon Ti with RGB illumination under ×10 or ×20 magnification.

### TE expression quantification

In addition to grouped germline samples collected for mRNA-seq and small RNA-seq, we collected single distal germline (four for each condition) into 10 µl 0.2% Triton X100 with RNase inhibitor (final concentration 1 U µl<sup>-1</sup>). mRNA libraries for directional RNA-seq were prepared using the SMARTer Apollo System and were sequenced (150-nt single-end) on the Illumina NovaSeq platform. Reads from germline mRNA-seq were mapped to the *C. elegans* RepBase database (<https://www.girinst.org/server/RepBase/protected/repeatmaskerlibraries/RepBaseRepeatMaskerEdition-20181026.tar.gz>) using Bowtie. Raw counts were then normalized on the total number of mapping reads and multiplied by 1,000,000, obtaining expression values indicated as reads per million mapped reads (RPM). Transposon type was determined according to RepBase's annotation.

### Statistics and reproducibility

No statistical method was used to predetermine sample size. Sample sizes were chosen according to professional standards of the field for individual assays. For RNA-seq, three biological replicates were performed for each condition per genotype<sup>83</sup>. About 200 distal germlines were collected in each replicate<sup>84</sup>. No RNA-seq library was excluded from the analyses. In lifespan assays, each group contains 50–100 worms and at least two biological replicates were performed for each condition and genotype<sup>85</sup>. To compare body size changes, 30–50 worms per genotype per condition were measured<sup>12</sup>.

Reported results were consistently replicated across multiple experiments. Postmating body size measurements and lifespan assays were repeated twice if mating causes significant shrinking and early death. In the case of treatments that brought protection against mating-induced shrinking or early death, at least three replicates were performed to confirm the effect. During initial RNAi screen of candidates, the names of the targeting gene were blinded. The investigators were not blinded in follow-up lifespan assays, since only two to three groups of worms were tested each time. However, for these follow-up lifespan assays, the number of worms for each group was increased from around 50 (in blinded lifespan assays) to over 100. When quantifying the P granule intensities of mated and unmated worms, images were scored blindly. No randomization was necessary for this study

because mated and unmated worms of specific genotype/treatment were always compared with each other.

Lifespan data were plotted as Kaplan–Meier survival curves and statistical analyses were performed using the log-rank (Mantel–Cox) test and two-way ANOVA. For body size measurements and fluorescence intensity quantification, two-tailed *t*-test was used for all comparisons to determine statistical significance in this study. Detailed information of each assay can be found in the corresponding figure legends.

Source Data for sequencing data and statistics displayed in the main figures are provided as Supplementary Files.

### Reporting summary

Further information on research design is available in the Nature Portfolio Reporting Summary linked to this article.

### Data availability

All RNA-seq reads are available on NCBI Sequence Read Archive (PRJNA892981). The microarray data were retrieved from previous publications<sup>34,61</sup> and are available at <http://puma.princeton.edu>. All other data supporting the findings of this study are available from the corresponding author upon request. Source data are provided with this paper.

### References

- Wade, G. N. & Schneider, J. E. Metabolic fuels and reproduction in female mammals. *Neurosci. Biobehav. Rev.* **16**, 235–272 (1992).
- Chantranupong, L., Wolfson, R. L. & Sabatini, D. M. Nutrient-sensing mechanisms across evolution. *Cell* **161**, 67–83 (2015).
- Dupont, J. et al. Nutritional signals and reproduction. *Mol. Cell. Endocrinol.* **382**, 527–537 (2014).
- Efeyan, A., Comb, W. C. & Sabatini, D. M. Nutrient-sensing mechanisms and pathways. *Nature* **517**, 302–310 (2015).
- Templeman, N. M. & Murphy, C. T. Regulation of reproduction and longevity by nutrient-sensing pathways. *J. Cell Biol.* **217**, 93–106 (2018).
- Laws, K. M. & Drummond-Barbosa, D. Control of germline stem cell lineages by diet and physiology. *Results Probl. Cell Differ.* **59**, 67–99 (2017).
- Hsin, H. & Kenyon, C. Signals from the reproductive system regulate the lifespan of *C. elegans*. *Nature* **399**, 362–366 (1999).
- Cargill, S. L. et al. Age of ovary determines remaining life expectancy in old ovariectomized mice. *Aging Cell* **2**, 185–190 (2003).
- Min, K. J., Lee, C. K. & Park, H. N. The lifespan of Korean eunuchs. *Curr. Biol.* **22**, R792–R793 (2012).
- Arantes-Oliveira, N. et al. Regulation of life-span by germline stem cells in *Caenorhabditis elegans*. *Science* **295**, 502–505 (2002).
- Flatt, T. et al. *Drosophila* germ-line modulation of insulin signaling and lifespan. *Proc. Natl Acad. Sci. USA* **105**, 6368–6373 (2008).
- Shi, C. & Murphy, C. T. Mating induces shrinking and death in *Caenorhabditis* mothers. *Science* **343**, 536–540 (2014).
- Shi, C., Runnels, A. M. & Murphy, C. T. Mating and male pheromone kill *Caenorhabditis* males through distinct mechanisms. *eLife* **6**, e23493 (2017).
- Shi, C. & Murphy, C. T. in *Current Topics in Developmental Biology* Vol. 144 (eds Jarriault, S. & Podbilewicz, B.) Ch. 11 (Academic Press, 2021).
- Ben-Zvi, A., Miller, E. A. & Morimoto, R. I. Collapse of proteostasis represents an early molecular event in *Caenorhabditis elegans* aging. *Proc. Natl Acad. Sci. USA* **106**, 14914–14919 (2009).
- O'Rourke, E. J. et al. *C. elegans* major fats are stored in vesicles distinct from lysosome-related organelles. *Cell Metab.* **10**, 430–435 (2009).

17. Alper, S. et al. The *Caenorhabditis elegans* germ line regulates distinct signaling pathways to control lifespan and innate immunity. *J. Biol. Chem.* **285**, 1822–1828 (2010).
18. Vilchez, D. et al. RPN-6 determines *C. elegans* longevity under proteotoxic stress conditions. *Nature* **489**, 263–268 (2012).
19. Lapierre, L. R. & Hansen, M. Lessons from *C. elegans*: signaling pathways for longevity. *Trends Endocrinol. Metab.* **23**, 637–644 (2012).
20. Berman, J. R. & Kenyon, C. Germ-cell loss extends *C. elegans* life span through regulation of *DAF-16* by *kri-1* and lipophilic-hormone signaling. *Cell* **124**, 1055–1068 (2006).
21. McCormick, M. et al. New genes that extend *Caenorhabditis elegans*' lifespan in response to reproductive signals. *Aging Cell* **11**, 192–202 (2012).
22. Goudeau, J. et al. Fatty acid desaturation links germ cell loss to longevity through NHR-80/HNF4 in *C. elegans*. *PLoS Biol.* **9**, e1000599 (2011).
23. Lapierre, L. R. et al. Autophagy and lipid metabolism coordinately modulate life span in germline-less *C. elegans*. *Curr. Biol.* **21**, 1507–1514 (2011).
24. Antebi, A. Regulation of longevity by the reproductive system. *Exp. Gerontol.* **48**, 596–602 (2013).
25. O'Rourke, E. J. & Ruvkun, G. MXL-3 and HLH-30 transcriptionally link lipolysis and autophagy to nutrient availability. *Nat. Cell Biol.* **15**, 668–676 (2013).
26. Ratnappan, R. et al. Germline signals deploy NHR-49 to modulate fatty-acid  $\beta$ -oxidation and desaturation in somatic tissues of *C. elegans*. *PLoS Genet.* **10**, e1004829 (2014).
27. Boulias, K. & Horvitz, H. R. The *C. elegans* microRNA *mir-71* acts in neurons to promote germline-mediated longevity through regulation of *DAF-16/FOXO*. *Cell Metab.* **15**, 439–450 (2012).
28. Kenyon, C. A pathway that links reproductive status to lifespan in *Caenorhabditis elegans*. *Ann. N. Y. Acad. Sci.* **1204**, 156–162 (2010).
29. Yamawaki, T. M. et al. The somatic reproductive tissues of *C. elegans* promote longevity through steroid hormone signaling. *PLoS Biol.* **8**, e1000468 (2010).
30. Gerisch, B. et al. A bile acid-like steroid modulates *Caenorhabditis elegans* lifespan through nuclear receptor signaling. *Proc. Natl Acad. Sci. USA* **104**, 5014–5019 (2007).
31. Pincus, Z., Mazer, T. C. & Slack, F. J. Autofluorescence as a measure of senescence in *C. elegans*: look to red, not blue or green. *Aging (Albany NY)* **8**, 889–898 (2016).
32. Maures, T. J. et al. Males shorten the life span of *C. elegans* hermaphrodites via secreted compounds. *Science* **343**, 541–544 (2014).
33. Shi, C., Booth, L. N. & Murphy, C. T. Insulin-like peptides and the mTOR-TFEB pathway protect *Caenorhabditis elegans* hermaphrodites from mating-induced death. *eLife* **8**, e46413 (2019).
34. Booth, L. N. et al. Males induce premature demise of the opposite sex by multifaceted strategies. *Nat. Aging* **2**, 809–823 (2022).
35. Reed, K. J. et al. Widespread roles for piRNAs and WAGO-class siRNAs in shaping the germline transcriptome of *Caenorhabditis elegans*. *Nucleic Acids Res.* **48**, 1811–1827 (2020).
36. Shen, Y. et al. A steroid receptor-microRNA switch regulates life span in response to signals from the gonad. *Science* **338**, 1472–1476 (2012).
37. Cohen-Berkman, M. et al. Endogenous siRNAs promote proteostasis and longevity in germline-less *Caenorhabditis elegans*. *eLife* **9**, e50896 (2020).
38. Klattenhoff, C. & Theurkauf, W. Biogenesis and germline functions of piRNAs. *Development* **135**, 3 (2008).
39. Aravin, A. A., Hannon, G. J. & Brennecke, J. The Piwi-piRNA pathway provides an adaptive defense in the transposon arms race. *Science* **318**, 761–764 (2007).
40. Brennecke, J. et al. Discrete small RNA-generating loci as master regulators of transposon activity in *Drosophila*. *Cell* **128**, 1089–1103 (2007).
41. Bagijn, M. P. et al. Function, targets, and evolution of *Caenorhabditis elegans* piRNAs. *Science* **337**, 574–578 (2012).
42. Belicard, T., Jareosettasin, P. & Sarkies, P. The piRNA pathway responds to environmental signals to establish intergenerational adaptation to stress. *BMC Biol.* **16**, 103 (2018).
43. Ouyang, J. P. T. et al. P granules protect RNA interference genes from silencing by piRNAs. *Dev. Cell* **50**, 716–728.e6 (2019).
44. Grishok, A. et al. Genes and mechanisms related to RNA interference regulate expression of the small temporal RNAs that control *C. elegans* developmental timing. *Cell* **106**, 23–34 (2001).
45. Ketting, R. F. et al. Dicer functions in RNA interference and in synthesis of small RNA involved in developmental timing in *C. elegans*. *Genes Dev.* **15**, 2654–2659 (2001).
46. Knight, S. W. & Bass, B. L. A role for the RNase III enzyme DCR-1 in RNA interference and germ line development in *Caenorhabditis elegans*. *Science* **293**, 2269–2271 (2001).
47. Han, T. et al. 26G endo-siRNAs regulate spermatogenic and zygotic gene expression in *Caenorhabditis elegans*. *Proc. Natl Acad. Sci. USA* **106**, 18674–18679 (2009).
48. Conine, C. C. et al. Argonautes ALG-3 and ALG-4 are required for spermatogenesis-specific 26G-RNAs and thermotolerant sperm in *Caenorhabditis elegans*. *Proc. Natl Acad. Sci. USA* **107**, 3588–3593 (2010).
49. Weick, E.-M. et al. PRDE-1 is a nuclear factor essential for the biogenesis of Ruby motif-dependent piRNAs in *C. elegans*. *Genes Dev.* **28**, 783–796 (2014).
50. Batista, P. J. et al. PRG-1 and 21U-RNAs interact to form the piRNA complex required for fertility in *C. elegans*. *Mol. Cell* **31**, 67–78 (2008).
51. Das, P. P. et al. Piwi and piRNAs act upstream of an endogenous siRNA pathway to suppress Tc3 transposon mobility in the *Caenorhabditis elegans* germline. *Mol. Cell* **31**, 79–90 (2008).
52. Wang, G. & Reinke, V. A *C. elegans* Piwi, PRG-1, regulates 21U-RNAs during spermatogenesis. *Curr. Biol.* **18**, 861–867 (2008).
53. Gu, W. et al. Distinct argonaute-mediated 22G-RNA pathways direct genome surveillance in the *C. elegans* germline. *Mol. Cell* **36**, 231–244 (2009).
54. Ashe, A. et al. piRNAs can trigger a multigenerational epigenetic memory in the germline of *C. elegans*. *Cell* **150**, 88–99 (2012).
55. Shen, E.-Z. et al. Identification of piRNA binding sites reveals the argonaute regulatory landscape of the *C. elegans* germline. *Cell* **172**, 937–951.e18 (2018).
56. Zhang, D. et al. The piRNA targeting rules and the resistance to piRNA silencing in endogenous genes. *Science* **359**, 587 (2018).
57. Wang, J. T. et al. Regulation of RNA granule dynamics by phosphorylation of serine-rich, intrinsically disordered proteins in *C. elegans*. *eLife* **3**, e04591 (2014).
58. Moore, R. S. et al. The role of the Cer1 transposon in horizontal transfer of transgenerational memory. *Cell* **184**, 4697–4712.e18 (2021).
59. Kim, K. W. et al. A neuronal piRNA pathway inhibits axon regeneration in *C. elegans*. *Neuron* **97**, 511–519.e6 (2018).
60. Weick, E.-M. & Miska, E. A. piRNAs: from biogenesis to function. *Development* **141**, 3458–3471 (2014).
61. Choi, L. S. et al. Oleic acid protects *Caenorhabditis* mothers from mating-induced death and the cost of reproduction. *Front. Cell Dev. Biol.* **9**, 690373 (2021).
62. Wu, W.-S. et al. piRTarBase: a database of piRNA targeting sites and their roles in gene regulation. *Nucleic Acids Res.* **47**, D181–D187 (2019).



63. Chou, K. C. & Shen, H. B. A new method for predicting the subcellular localization of eukaryotic proteins with both single and multiple sites: Euk-mPLoc 2.0. *PLoS ONE* **5**, e9931 (2010).
64. Almagro Armenteros, J. J. et al. SignalP 5.0 improves signal peptide predictions using deep neural networks. *Nat. Biotechnol.* **37**, 420–423 (2019).
65. Priyadarshini, M. et al. Reprogramming the piRNA pathway for multiplexed and transgenerational gene silencing in *C. elegans*. *Nat. Methods* **19**, 187–194 (2022).
66. Chikina, M. D. et al. Global prediction of tissue-specific gene expression and context-dependent gene networks in *Caenorhabditis elegans*. *PLoS Comput. Biol.* **5**, e1000417 (2009).
67. Kaletsky, R. et al. Transcriptome analysis of adult *Caenorhabditis elegans* cells reveals tissue-specific gene and isoform expression. *PLoS Genet.* **14**, e1007559 (2018).
68. Szklarczyk, D. et al. The STRING database in 2021: customizable protein–protein networks, and functional characterization of user-uploaded gene/measurement sets. *Nucleic Acids Res.* **49**, D605–D612 (2021).
69. Ingham, P. W., Nakano, Y. & Seger, C. Mechanisms and functions of Hedgehog signalling across the metazoa. *Nat. Rev. Genet.* **12**, 393–406 (2011).
70. Templeman, N. M. et al. CREB non-autonomously controls reproductive aging through Hedgehog/Patched signaling. *Dev. Cell* **54**, 92–105.e5 (2020).
71. Rodenfels, J. et al. Production of systemically circulating Hedgehog by the intestine couples nutrition to growth and development. *Genes Dev.* **28**, 2636–2651 (2014).
72. Rallis, A. et al. Hedgehog signaling modulates glial proteostasis and lifespan. *Cell Rep.* **30**, 2627–2643.e5 (2020).
73. Lee, M. J. et al. Hedgehog pathway inhibitor saridegib (IPI-926) increases lifespan in a mouse medulloblastoma model. *Proc. Natl Acad. Sci. USA* **109**, 7859 (2012).
74. Ozata, D. M. et al. PIWI-interacting RNAs: small RNAs with big functions. *Nat. Rev. Genet.* **20**, 89–108 (2019).
75. Rojas-Ríos, P. & Simonelig, M. piRNAs and PIWI proteins: regulators of gene expression in development and stem cells. *Development* **145**, dev161786 (2018).
76. Lee, E. J. et al. Identification of piRNAs in the central nervous system. *RNA* **17**, 1090–1099 (2011).
77. Rajasethupathy, P. et al. A role for neuronal piRNAs in the epigenetic control of memory-related synaptic plasticity. *Cell* **149**, 693–707 (2012).
78. Heimbucher, T. et al. PQM-1 controls hypoxic survival via regulation of lipid metabolism. *Nat. Commun.* **11**, 4627 (2020).
79. Campbell, A. C. & Updike, D. L. CSR-1 and P granules suppress sperm-specific transcription in the *C. elegans* germline. *Development* **142**, 1745–1755 (2015).
80. Tusher, V. G., Tibshirani, R. & Chu, G. Significance analysis of microarrays applied to the ionizing radiation response. *Proc. Natl Acad. Sci. USA* **98**, 5116–5121 (2001).
81. Petropavlovskiy, A. A. et al. A quantitative imaging-based protocol for yeast growth and survival on agar plates. *STAR Protoc.* **1**, 100182 (2020).
82. Gelino, S. et al. Intestinal autophagy improves healthspan and longevity in *C. elegans* during dietary restriction. *PLoS Genet.* **12**, e1006135 (2016).
83. Amrit, F. R. G. & Ghazi, A. Transcriptomic analysis of *C. elegans* RNA sequencing data through the Tuxedo Suite on the Galaxy Project. *J. Vis. Exp.* **122**, 55473 (2017).
84. Robert, V. J. et al. *Caenorhabditis elegans* SET1/COMPASS maintains germline identity by preventing transcriptional deregulation across generations. *Front. Cell Dev. Biol.* **8**, 561791 (2020).
85. Shaw, W. M. et al. The *C. elegans* TGF-beta Dauer pathway regulates longevity via insulin signaling. *Curr. Biol.* **17**, 1635–1645 (2007).
86. Angeles-Albores, D. et al. Tissue enrichment analysis for *C. elegans* genomics. *BMC Bioinf.* **17**, 366 (2016).

## Acknowledgements

We thank members of C.T.M.'s laboratory for critically reading the manuscript and valuable feedback. We thank the *Caenorhabditis* Genetics Center (CGC) for strains, the Genomics Core Facility at Princeton University and BioRender for model figure (Figs. 1e, 4a, 6g,h) design software. This work was supported by the Howard Hughes Medical Institute Faculty Scholar Award (55108545) to C.T.M., a Global Consortium for Reproductive Longevity and Equality Scholar Award to C.T.M. (GCRLE-0220) and the Simons Foundation (Simons Collaboration on the Plasticity and the Aging Brain, 811235SPI).

## Author contributions

This study was designed by C.S. and C.T.M. C.S. performed the experiments. Data were analyzed by C.S. and C.T.M. The manuscript was written by C.S. and C.T.M.

## Competing interests

The authors declare no competing interests.

## Additional information

**Extended data** is available for this paper at <https://doi.org/10.1038/s43587-022-00329-2>.

**Supplementary information** The online version contains supplementary material available at <https://doi.org/10.1038/s43587-022-00329-2>.

**Correspondence and requests for materials** should be addressed to Cheng Shi or Coleen T. Murphy.

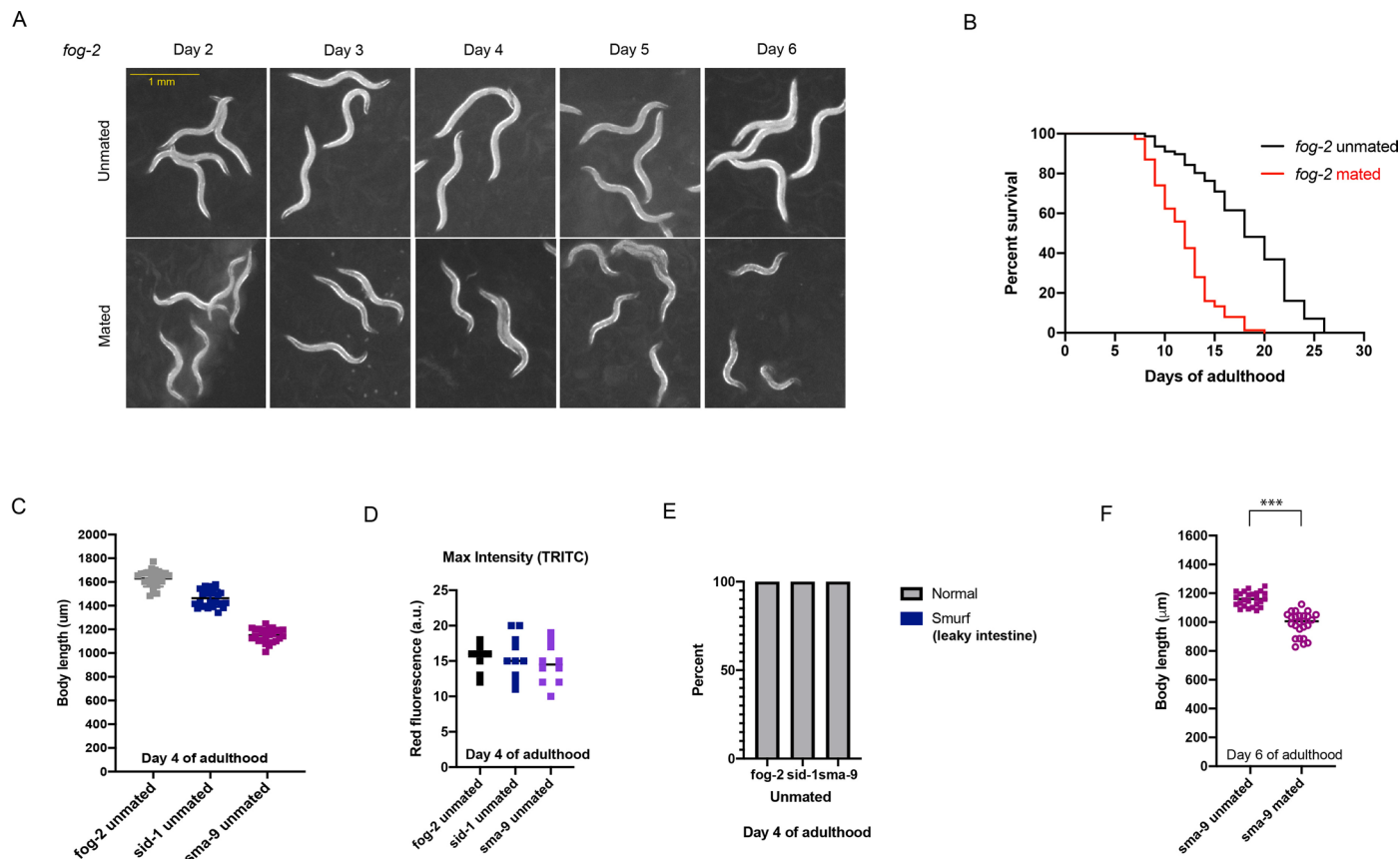
**Peer review information** *Nature Aging* thanks the anonymous reviewers for their contribution to the peer review of this work.

**Reprints and permissions information** is available at [www.nature.com/reprints](http://www.nature.com/reprints).

**Publisher's note** Springer Nature remains neutral with regard to jurisdictional claims in published maps and institutional affiliations.

**Open Access** This article is licensed under a Creative Commons Attribution 4.0 International License, which permits use, sharing, adaptation, distribution and reproduction in any medium or format, as long as you give appropriate credit to the original author(s) and the source, provide a link to the Creative Commons license, and indicate if changes were made. The images or other third party material in this article are included in the article's Creative Commons license, unless indicated otherwise in a credit line to the material. If material is not included in the article's Creative Commons license and your intended use is not permitted by statutory regulation or exceeds the permitted use, you will need to obtain permission directly from the copyright holder. To view a copy of this license, visit <http://creativecommons.org/licenses/by/4.0/>.

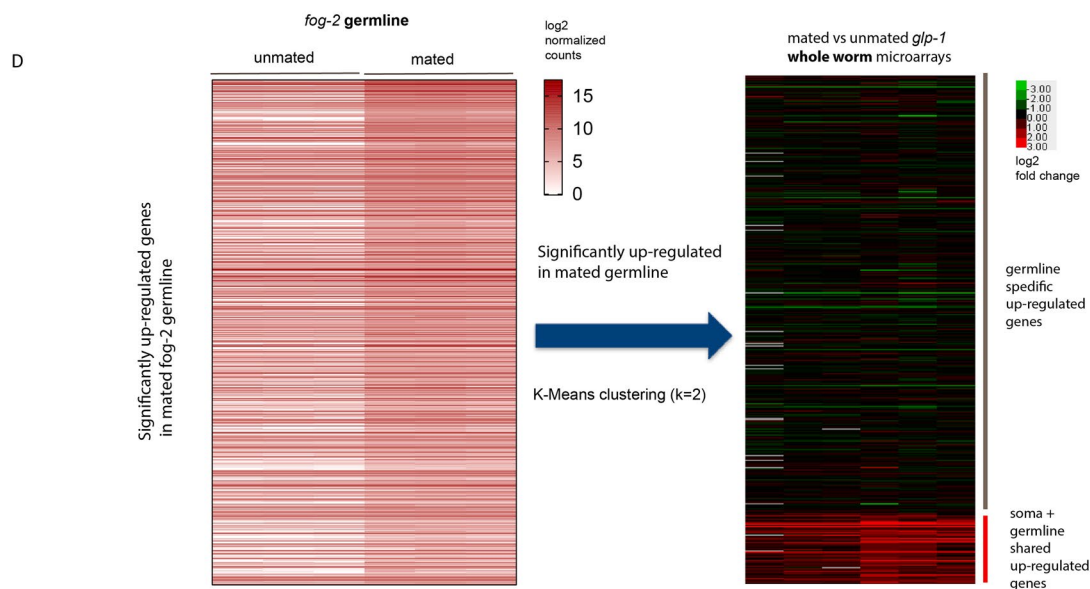
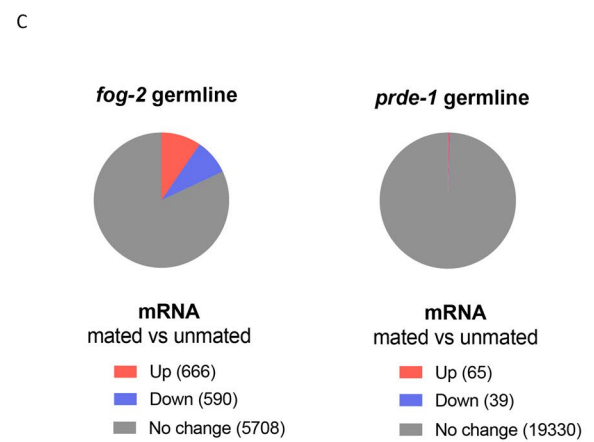
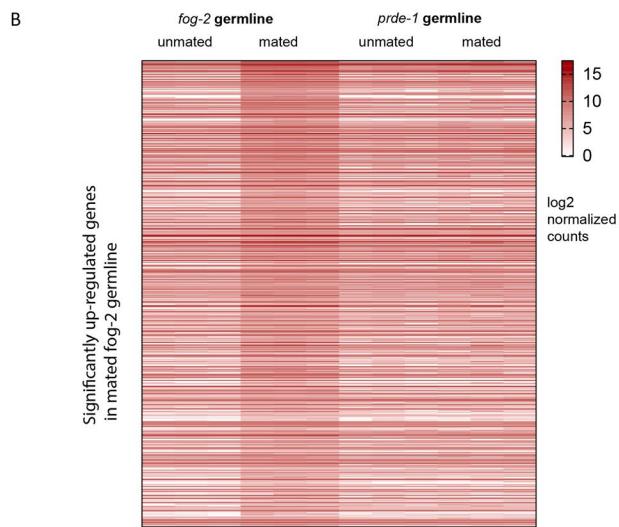
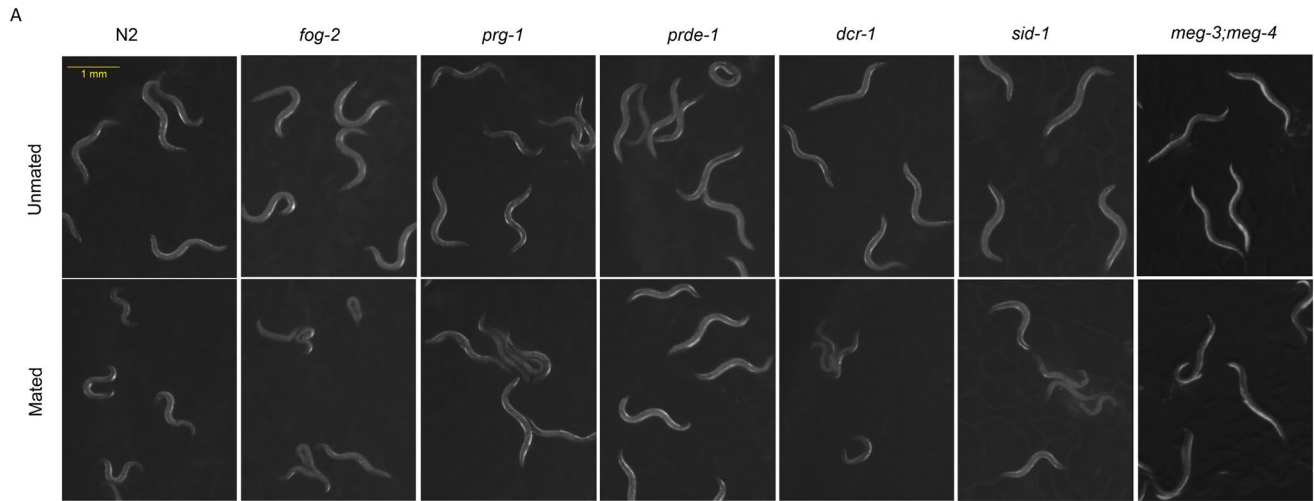
© The Author(s) 2023



### Extended Data Fig. 1 | Mating induces shrinking and other aging phenotypes that are independent of developmental body size regulation.

**A**) Representative pictures of the unmated and mated hermaphrodites from Day 2 – Day 6 of adulthood. Mating occurs on Day 1 for 24 hours. **B**) Representative lifespan of unmated and mated *fog-2* hermaphrodites. Unmated:  $18.2 \pm 0.6$  days,  $n = 85$ ; mated:  $12.0 \pm 0.3$  days,  $n = 83$ ,  $p < 0.001$ . Lifespan results are presented as mean values  $\pm$  std error for all the lifespan assays in this study.  $n$  represents the number of biologically independent animals in the lifespan assay. Significance was determined by Log-rank (Mantel–Cox) test for lifespan comparisons. **C**) Quantification of unmated Day 4 worms with various body sizes (wildtype *fog-2*, *sid-1*, and *sma-9*). Unmated *fog-2*:  $1630 \pm 68 \mu\text{m}$  ( $n = 25$ ), unmated *sid-1*:

$1462 \pm 72 \mu\text{m}$  ( $n = 25$ ), unmated *sma-9*:  $1151 \pm 58 \mu\text{m}$  ( $n = 25$ ). **D**) Quantification of maximum red autofluorescence of unmated wildtype *fog-2*, *sid-1*, and *sma-9* worms. No difference was observed despite their different body sizes. *fog-2*:  $15.4 \pm 1.9$  a.u. ( $n = 10$ ), *sid-1*:  $15.6 \pm 3.1$  a.u. ( $n = 10$ ), *sma-9*:  $14.6 \pm 2.8$  a.u. ( $n = 10$ ). Red autofluorescence data are presented as maximum values  $\pm$  SD.  $n$  represents the number of biologically independent animals. **E**) Quantification of intestinal leakage of these unmated Day 4 wildtype *fog-2*, *sid-1*, and *sma-9* hermaphrodites. 50 worms were scored for each genotype. **F**) Body size measurement of mated and unmated *sma-9* (*wk55*) mutants. Day 6 unmated *sma-9*:  $1160 \pm 49 \mu\text{m}$  ( $n = 25$ ), mated *sma-9*:  $989 \pm 82 \mu\text{m}$  ( $n = 25$ ), \*\*\*  $p < 0.0001$ .

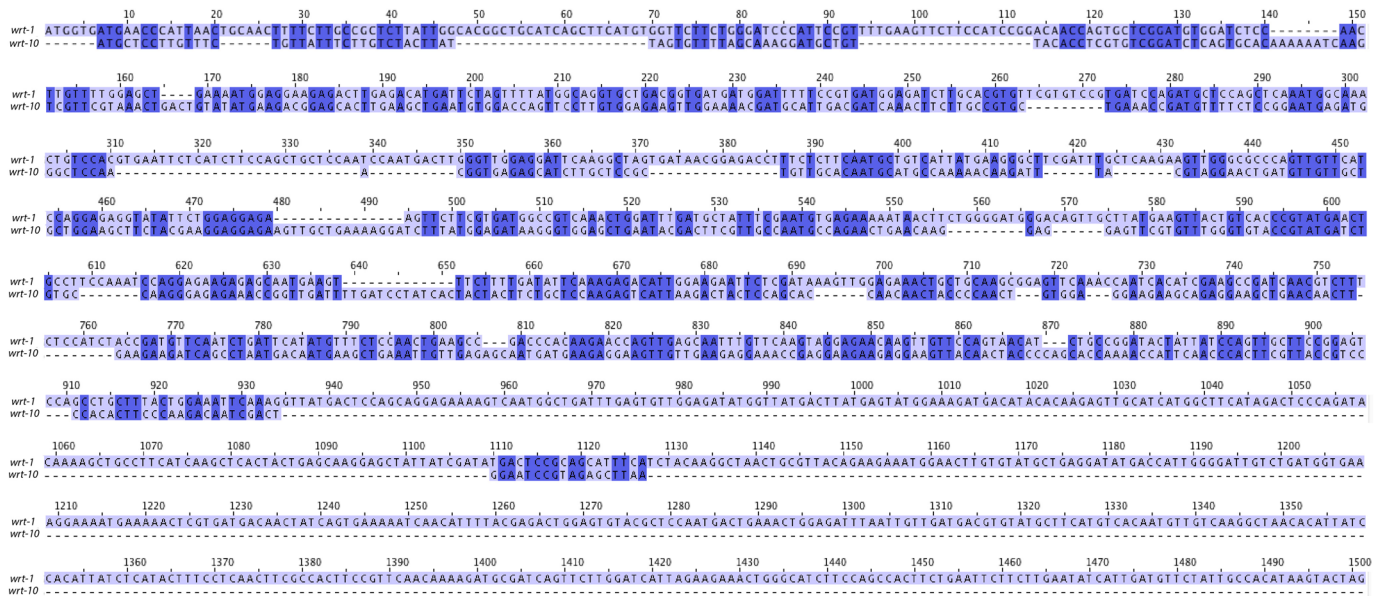


Extended Data Fig. 2 | See next page for caption.

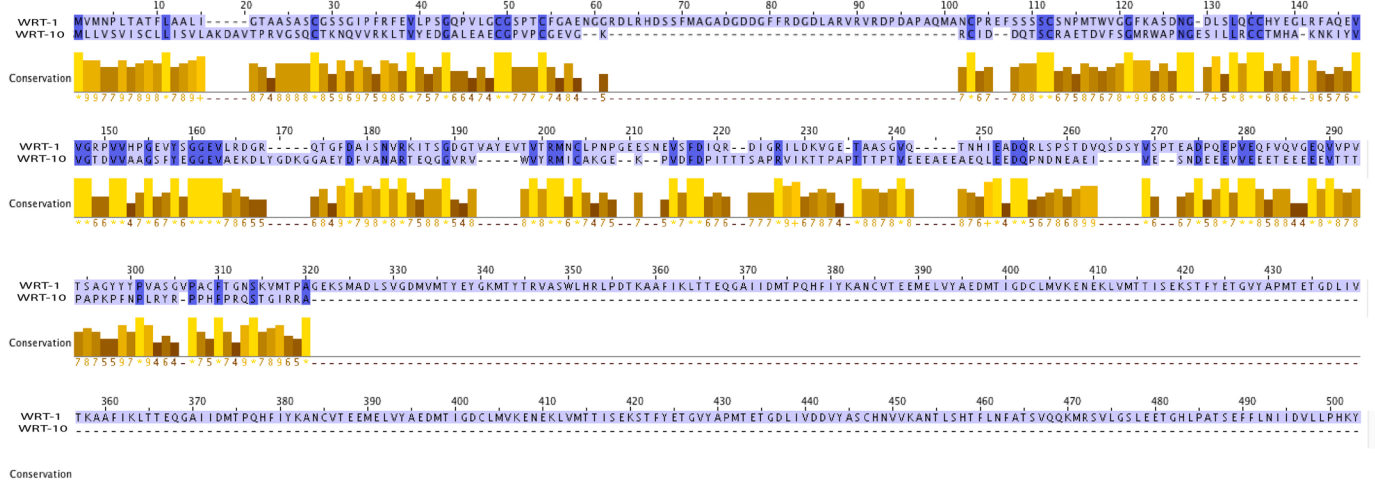
**Extended Data Fig. 2 | piRNA pathway mutants are resistant to mating-induced shrinking and lack transcriptional responses in the germline.** A) Representative pictures of the unmated and mated hermaphrodites related to different small RNA pathways on Day 6/7 of adulthood. At least 20-30 worms (n) were measured for each condition and genotype. See Fig. 3A (N2, *dcr-1*, *sid-1*), Fig. 3B (*fog-2*, *prg-1*, *prde-1*), Fig. 3E (*meg-3*; *meg-4*) for comparisons and statistics. B) Heatmap of genes that are significantly up-regulated in mated *fog-2*

germline. The data are displayed as log<sub>2</sub>(normalized counts). Mating-induced up-regulation in expression is completely abolished in piRNA pathway-deficient *prde-1* germlines. C) Pie chart summary of mating-induced expressional changes in normal functional *fog-2* germline (left) and piRNA pathway deficient *prde-1* germline (right). D) K-Means (k = 2) clustering separates the significantly up-regulated genes in *fog-2* mated germline to germline-specific transcriptional response and generic transcriptional response to mating.

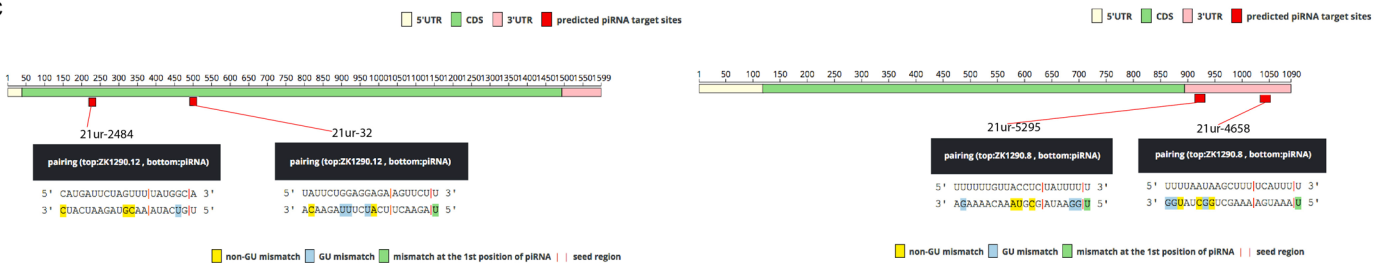
A



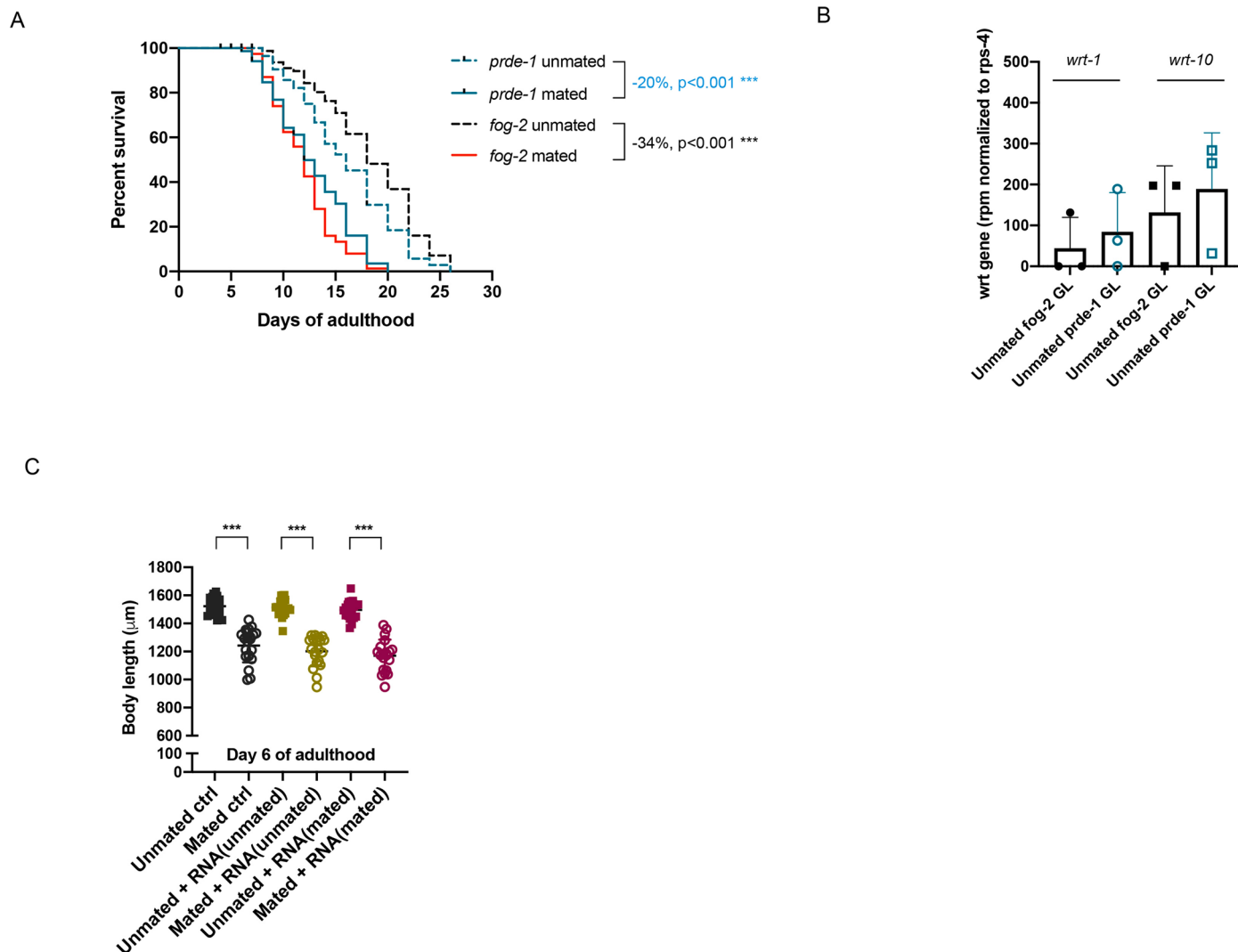
B



C



**Extended Data Fig. 3 | Sequence homology of *wrt-1* and *wrt-10*.** A) Comparison of *wrt-1* and *wrt-10* cDNA sequences using Clustal Omega (<https://www.ebi.ac.uk/Tools/msa/clustalo/>). B) Comparison of WRT-1 and WRT-10 protein sequences using Clustal Omega. C) *wrt-1*- (left) and *wrt-10*- (right) targeting piRNAs: sequences and predicted binding sites. Figures were modified from piRTarBase.



**Extended Data Fig. 4 | Inhibiting piRNA pathway and Hedgehog signaling largely ameliorates mating-induced early death.** A) Lifespans of mated and unmated worms with defective piRNA pathway and control. *fog-2* unmated ctrl:  $18.2 \pm 0.6$  days,  $n = 85$ , *fog-2* mated ctrl:  $12.0 \pm 0.3$  days,  $n = 83$ ,  $p < 0.001$ ; *prde-1* unmated ctrl:  $16.1 \pm 0.5$  days,  $n = 89$ , *prde-1* mated ctrl:  $12.8 \pm 0.5$  days,  $n = 77$ ,  $p < 0.001$ . Significance was determined by Log-rank (Mantel-Cox) test. B) Expression levels of *wrt-1* and *wrt-10* genes in the germline of unmated *fog-2* and *prde-1* worms (three biological replicates in total, each replicate contains a pool of 200 dissected germlines). Read counts were normalized to housekeeping gene *rps-4* in each sample. Expression data are presented as mean values  $\pm$  SD. Expression level of *wrt-1* in unmated *fog-2* germline:  $44 \pm 76$  rpm (reads per million reads), unmated *prde-1* germline:  $84 \pm 96$  rpm. Expression level of *wrt-10*

in unmated *fog-2* germline:  $132 \pm 114$  rpm, unmated *prde-1* germline:  $189 \pm 137$  rpm. C) Mating-induced shrinking is not affected by large amounts of extracted total RNA from unmated or mated worms. 2  $\mu\text{g}$  of total RNA of each type with RNase inhibitor was seeded on plate for the assay. Worms were transferred every two days onto freshly seeded plates with total RNA supplementation. Body size measurements: unmated control:  $1524 \pm 66$   $\mu\text{m}$  ( $n = 19$ ), mated control:  $1242 \pm 119$   $\mu\text{m}$  ( $n = 21$ ),  $***p < 0.001$ ; unmated with total RNA extracted from unmated whole worms:  $1513 \pm 63$   $\mu\text{m}$  ( $n = 20$ ), mated with total RNA extracted from unmated whole worms:  $1202 \pm 107$   $\mu\text{m}$  ( $n = 20$ ),  $***p < 0.001$ ; unmated with total RNA extracted from mated whole worms:  $1496 \pm 64$   $\mu\text{m}$  ( $n = 20$ ), mated with total RNA extracted from mated whole worms:  $1170 \pm 115$   $\mu\text{m}$  ( $n = 20$ ),  $***p < 0.001$ .

## Reporting Summary

Nature Portfolio wishes to improve the reproducibility of the work that we publish. This form provides structure for consistency and transparency in reporting. For further information on Nature Portfolio policies, see our [Editorial Policies](#) and the [Editorial Policy Checklist](#).

### Statistics

For all statistical analyses, confirm that the following items are present in the figure legend, table legend, main text, or Methods section.

n/a Confirmed

- The exact sample size ( $n$ ) for each experimental group/condition, given as a discrete number and unit of measurement
- A statement on whether measurements were taken from distinct samples or whether the same sample was measured repeatedly
- The statistical test(s) used AND whether they are one- or two-sided  
*Only common tests should be described solely by name; describe more complex techniques in the Methods section.*
- A description of all covariates tested
- A description of any assumptions or corrections, such as tests of normality and adjustment for multiple comparisons
- A full description of the statistical parameters including central tendency (e.g. means) or other basic estimates (e.g. regression coefficient) AND variation (e.g. standard deviation) or associated estimates of uncertainty (e.g. confidence intervals)
- For null hypothesis testing, the test statistic (e.g.  $F$ ,  $t$ ,  $r$ ) with confidence intervals, effect sizes, degrees of freedom and  $P$  value noted  
*Give  $P$  values as exact values whenever suitable.*
- For Bayesian analysis, information on the choice of priors and Markov chain Monte Carlo settings
- For hierarchical and complex designs, identification of the appropriate level for tests and full reporting of outcomes
- Estimates of effect sizes (e.g. Cohen's  $d$ , Pearson's  $r$ ), indicating how they were calculated

*Our web collection on [statistics for biologists](#) contains articles on many of the points above.*

### Software and code

Policy information about [availability of computer code](#)

Data collection

Data analysis

For manuscripts utilizing custom algorithms or software that are central to the research but not yet described in published literature, software must be made available to editors and reviewers. We strongly encourage code deposition in a community repository (e.g. GitHub). See the Nature Portfolio [guidelines for submitting code & software](#) for further information.

### Data

Policy information about [availability of data](#)

All manuscripts must include a [data availability statement](#). This statement should provide the following information, where applicable:

- Accession codes, unique identifiers, or web links for publicly available datasets
- A description of any restrictions on data availability
- For clinical datasets or third party data, please ensure that the statement adheres to our [policy](#)

All RNA sequencing datasets are deposited at NCBI BioProject BioProject ID PRJNA892981. We have made the request to make the datasets publicly available.

## Field-specific reporting

Please select the one below that is the best fit for your research. If you are not sure, read the appropriate sections before making your selection.

Life sciences       Behavioural & social sciences       Ecological, evolutionary & environmental sciences

For a reference copy of the document with all sections, see [nature.com/documents/nr-reporting-summary-flat.pdf](https://www.nature.com/documents/nr-reporting-summary-flat.pdf)

## Life sciences study design

All studies must disclose on these points even when the disclosure is negative.

Sample size	Sample sizes were chosen according to professional standards of the field for individual assays. For RNA-sequencing, three biological replicates were performed for each condition/genotype (Amrit and Ghazi 2017). About 200 distal germlines were collected in each replicate (Robert et al., 2020). In lifespan assays, each group contains 50-100 worms, at least two biological replicates were performed for each condition/genotype (Shaw et al., 2007). To compare body size changes, 30-50 worms per genotype/condition were measured (Shi and Murphy, 2014). Detailed information regarding sample sizes of lifespan assays and body size measurements can be found in figure legends.
Data exclusions	Data were not excluded from analysis.
Replication	Reported results were consistently replicated across multiple experiments. Most experiments (body size measurements and lifespan assays) were repeated twice if mating causes significant shrinking and early death. In the case of treatments which brought protection against mating-induced shrinking or early death, at least three replicates were performed to confirm the effect.
Randomization	No randomization was necessary for this study because mated and unmated worms of specific genotype/treatment were always compared with each other.
Blinding	During initial RNAi screen of candidates, the names of the targeting gene were blinded. The investigators were not blinded in follow-up lifespan assays, since only two-three groups of worms were tested each time. However, for these follow-up lifespan assays, the number of worms for each group was increased from around 50 (in blinded lifespan assays) to over 100. When quantifying the P granule intensities of mated and unmated worms, images were scored blindly.

## Reporting for specific materials, systems and methods

We require information from authors about some types of materials, experimental systems and methods used in many studies. Here, indicate whether each material, system or method listed is relevant to your study. If you are not sure if a list item applies to your research, read the appropriate section before selecting a response.

### Materials & experimental systems

n/a	Involved in the study
<input checked="" type="checkbox"/>	<input type="checkbox"/> Antibodies
<input checked="" type="checkbox"/>	<input type="checkbox"/> Eukaryotic cell lines
<input checked="" type="checkbox"/>	<input type="checkbox"/> Palaeontology and archaeology
<input type="checkbox"/>	<input checked="" type="checkbox"/> Animals and other organisms
<input checked="" type="checkbox"/>	<input type="checkbox"/> Human research participants
<input checked="" type="checkbox"/>	<input type="checkbox"/> Clinical data
<input checked="" type="checkbox"/>	<input type="checkbox"/> Dual use research of concern

### Methods

n/a	Involved in the study
<input checked="" type="checkbox"/>	<input type="checkbox"/> ChIP-seq
<input checked="" type="checkbox"/>	<input type="checkbox"/> Flow cytometry
<input checked="" type="checkbox"/>	<input type="checkbox"/> MRI-based neuroimaging

## Animals and other organisms

Policy information about [studies involving animals](#); [ARRIVE guidelines](#) recommended for reporting animal research

Laboratory animals	C. elegans lab strains were used in this study. Detailed information (strain name, genotype, and sources) regarding each strain can be found in Material and Methods section. All the body size and lifespan experiments were performed using hermaphrodites. Young males (Day 1 - Day 2 of adulthood) were used only for mating. Hermaphrodites were mated on Day 1 of adulthood for 2 days and were separated from males on Day 3 and monitored throughout their lifespan.
Wild animals	This study did not involve wild animals.
Field-collected samples	No field collected samples were used in the study.
Ethics oversight	This study did not require an ethical approval.

Note that full information on the approval of the study protocol must also be provided in the manuscript.